Engineered common environmental effects on multitransistor systems

Uthpala N. Ekanayake [1,*] Sarath D. Gunapala [2] and Malin Premaratne [1,†]

[1]*Advanced Computing and Simulation Laboratory (AχL), Department of Electrical and Computer Systems Engineering, Monash University, Clayton, Victoria 3800, Australia*

[2]*Jet Propulsion Laboratory, California Institute of Technology, Pasadena, California 91109, USA*

In this paper, we analyze the impact of physically large baths used in terminals of thermal multitransistor systems formed using two-level systems (TLSs). In particular, we simulate the effects of a two-transistor system introduced as a thermal Darlington pair (DP). The size and proximity of the baths can cause multiple interactions with the transistor terminals represented by the TLS, not just the TLS directly connected to them. Such interactions can ultimately suppress the heat flows or impair the transistor action. However, we demonstrate that the DP model can achieve more than a 50% increase in heat flows. Using the engineered interactions leading to the correlated TLS-thermal bath interactions, we establish an incoherent (no quantum coherence in the density matrix at the steady state) yet correlated (joint excitation of two TLSs due to bath interaction) heat transfer model to a two-transistor arrangement in a substrate. This model helps us to interpret the environmental effects on the device by treating the common environment as separate thermal baths and all the transitions in the system as independent. We also show that this model can be mapped to contain dark-states. These dark-states can provide an external channel for transistor switching. We use this knowledge to design thermal counterparts of electronic AND and OR gates, and to study their switching time and operation, paving the way to realizing thermal logic gates.

I. INTRODUCTION

Over the years, nanotechnology has allowed the miniaturization and cost reduction of electronic components as a consequence of technological improvements in areas such as two-dimensional (2D) electronics based on graphene, organic electronics, memristors, spintronics, etc. The ability to manipulate such quantum resources in the electronic industry will be fruitful in building novel devices aimed at particular applications. One such potential application is controlling the thermal energy created inside nanoscale devices. Modern-day electronics can achieve better energy routing in circuits as a result of prospective quantum research. Joulain *et al.* [1] first demonstrated that thermal energy (heat) can be regulated and amplified, similar to electricity, via a thermal counterpart of an electronic bipolar transistor. There is a possibility in future to realize this kind of a model using quantum nanoparticles. The development of such works, including the thermal counterparts of a diode [2], a thermal gate similar to a field-effect transistor (FET) [3], a thermal rectifier [4], various improved models of thermal transistors [1,3,5–8], and a two-transistor model [9], demonstrates a potential for developing much more advanced energy management schemes in years to come. They can be beneficial for future energy harvesting/energy storage devices. The physical fabrication of these devices can be achievable as a result of the ongoing research in nanotechnology that includes metamaterials [10], nanoparticles, nanostructures, superconducting circuits [11–21], and spasers [22].

Quantum thermal devices are formulated based on models and approximations in quantum mechanics and open quantum dynamics. They are represented by systems that interact with an environment comprising thermal reservoirs under weak system-bath interactions. A quantum device that couples to an environment undergoes two phenomena: dissipation, where the irreversible loss of energy happens, and decoherence, which is the loss of coherence [23]. The heat-transfer process in the quantum system is interpreted based on these two incidents. In quantum systems, features such as quantum coherence are susceptible to noise. Quantum coherence can be described as a property in objects whose wavelike properties can be interfered with to form a single state with the superposition of two states [24]. However, this can get destroyed quickly via interactions with thermal baths. Coherence can be lost over time if such systems are not perfectly isolated.

The literature shows how manipulating quantum coherence aids in enhancing the efficiency of thermal devices [25–32]. To minimize the effects of decoherence, it is possible to use quantum reservoir engineering and control. Reservoir engineering includes minimizing the parameters where decoherence occurs. This can be achieved by changing the thermal baths' spectral densities or using the existing dissipative sources, such as thermal baths, to create entangled states in the system. Manzano *et al.* [33] discovered that by treating thermal baths as a common environment and carefully manipulating the system-bath interactions, it is possible to tune a quantum refrigerator to a dark-state. In their study, this

*uthpala.ekanayake@monash.edu

†malin.premaratne@monash.edu

ultimately preserved quantum coherence and improved the device's thermal efficiency. Furthermore, they developed an incoherent yet correlated model for the quantum refrigerator where common baths were treated as separate baths. Liu *et al.* [34] studied such common environmental effects and tuned their transistor model to a dark-state. The dark-state provided an additional channel to the transistor, so a laser field was used to change the magnitude of heat currents while maintaining the transistor amplification rate constant. The literature also discusses how the dark-states can be used to preserve quantum coherence.

We aspire to study engineered common environmental effects and the possibility of realizing additional applications in multitransistor arrangements. An analysis of this nature can be helpful in understanding the possible changes to the transistor action and the device performance due to environmental effects. Transistor models are connected to enormous baths to maintain their terminals at regulated temperatures. These terminals comprise two-level systems (TLSs) coupled to the thermal baths. The use of such physically large baths will not guarantee that the TLSs are separated enough to avoid multiple interactions from baths that are not directly coupled. Inspired by the current research in the literature on individual quantum systems, we explore the changes that can happen in a multitransistor model as it undergoes such multiple interactions. We study how an engineered environmental interaction affects the overall performance of a two-transistor model, particularly a thermal Darlington pair (DP). For this analysis, we establish an incoherent yet correlated heat-transfer model to the DP arrangement in a substrate. The incoherent-correlated model implies that at a steady state the system is not decoherence-free; however, the TLSs are correlated and there is a possibility of creating additional channels for heat transfer. An advantage of this model is that we can treat a common environment as separate baths and treat all the transitions induced in the system independently. The model can also be mapped to contain dark-states achieved via correlated TLSs. We show that it is possible to enhance the heat flows in the DP operating temperature range by appropriately configuring the model parameters. We improve the DP introduced in Wijesekara *et al.* [9] by incorporating multibath interactions induced in the system. Later we provide different arrangements where two transistors can be connected, we tune these systems to contain dark-states, and we use them to identify the thermal equivalent of AND and OR gates.

This paper is organized as follows. In Sec. II, we describe a multitransistor model for a DP, and we show how it can be realized using two separate transistors. Next, in Sec. III, we provide an interpretation of possible engineered interactions for a system coupled to thermal baths. In Sec. IV, we describe the formalism that incorporates environmental effects to the system. In Sec. V, we discuss the occurrence of quantum entanglement and how it preserves quantum coherence via dark-states. In Sec. VI, we discuss an incoherent yet correlated model to the multitransistor system, and we show how it can be combined to realize the DP. Then we use the multitransistor system to tune to contain dark-states. In Sec. VII, we discuss the possibility of realizing thermal logic gates. Finally, in Sec. VIII, we present our conclusion, including the models' limitations.
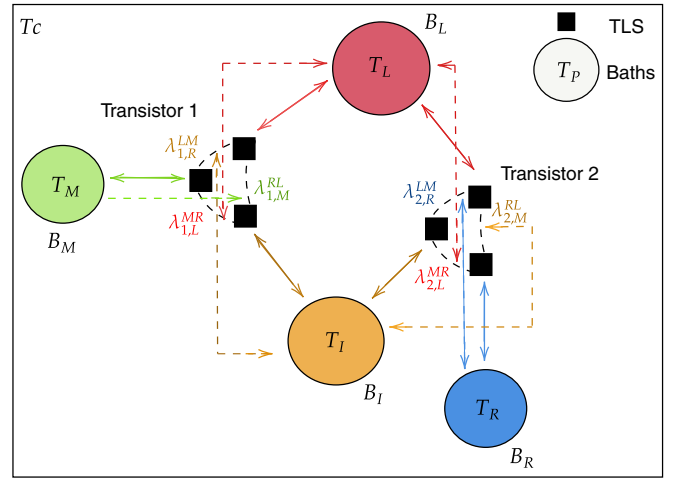
FIG. 1. Thermal Darlington pair arrangement with three TLSs as terminals interacting with reservoirs: B_L, B_M, B_I, and B_R, each with temperature T_L, T_M, T_I, and T_R. The substrate temperature is given by T_c. The direct interactions are shown by solid lines, and the indirect interactions (interactions from the same bath to the adjacent pair of TLSs) described by coupling constants $\lambda_{1,L}^{MR}$, $\lambda_{1,M}^{RL}$, $\lambda_{1,R}^{LM}$, $\lambda_{2,L}^{MR}$, $\lambda_{2,M}^{RL}$, $\lambda_{2,R}^{LM}$ are shown by dashed lines.

II. MULTI-TRANSISTOR MODEL

We discuss how common environmental effects affect multitransistor models. We visualize these effects via a simulation, particularly for a two-transistor model, with possible extensions to the multitransistors. We represent the terminals of the transistors as TLSs coupled to baths. We improve the previous model of the DP by Wijesekara *et al.* [9] to incorporate engineered environmental effects. This system comprises two transistors, each with three coupled TLSs, having one of two quantum states, namely spin up $|\uparrow\rangle$ or spin down $|\downarrow\rangle$. We provide a representation of the DP arrangement in Fig. 1. It comprises six TLSs, three reservoirs with fixed temperatures T_L, T_M, T_R, and an intermediate bath whose temperature T_I depends on the system's dynamics. The Hilbert space for each transistor ($s \in \{1, 2\}$) is spanned by the tensor product space of three individual TLSs, resulting in a composite system with 16 eigenstates. Each transistor comprises eight eigenstates given by

$$
\begin{aligned}
|1\rangle^s &= |\uparrow \ \uparrow\uparrow\rangle^s, & |5\rangle^s &= |\downarrow \ \uparrow\uparrow\rangle^s, \\
|2\rangle^s &= |\uparrow \ \uparrow\downarrow\rangle^s, & |6\rangle^s &= |\downarrow \ \uparrow\downarrow\rangle^s, \\
|3\rangle^s &= |\uparrow \ \downarrow\uparrow\rangle^s, & |7\rangle^s &= |\downarrow \ \downarrow\uparrow\rangle^s, \\
|4\rangle^s &= |\uparrow \ \downarrow\downarrow\rangle^s, & |8\rangle^s &= |\downarrow \ \downarrow\downarrow\rangle^s.
\end{aligned}
\tag{1}
$$

We assume that the reservoirs B_L, B_M, B_I, and B_R are a part of a substrate, and they act as a common environment. The baths interact with their coupled TLS directly, and the interaction with its adjacent pair is indirect via a coupling constant $\lambda_{s,P}^{QR}(P, Q, R \in \{L, M, R\})$ (refer to Fig. 1). The direct system bath interactions are weak, and the indirect interactions are far weaker. To maintain consistency with the combined model of DP, we take $\lambda_{1,R}^{LM} = \lambda_{2,M}^{RL}$. We establish an interaction Hamiltonian in Sec. III to include these $\lambda_{s,P}^{QR}$ terms.
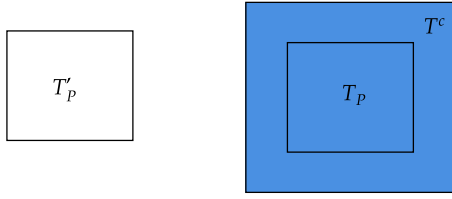
FIG. 2. This provides a visualization of bath temperatures. The bath temperature is given as T'_P when there is no information on the medium at which it is placed. When we have information on the substrate temperature T_c, the bath temperature is assigned as T_P.

Even though the baths act as a common environment, we should avoid them equilibrating to a common temperature. We can use an external mechanism and maintain them at their intended temperatures to cause the transistor action. At the steady state, the TLSs reach the equilibrium temperature with the directly coupled bath. We have three separate baths at the terminals of each transistor, which can behave as a common environment for the transistor. The temperature of each bath can be represented as in Fig. 2. When the substrate temperature and entropy are known as T_c and S_c, respectively, we assign the temperatures for the four separate reservoirs T_P as in Eq. (2), inspired by Refs. [35,36],

$$
\begin{aligned}
\frac{1}{T_L} &= \frac{1}{T'_L} - \left.\frac{\partial S_x}{\partial U_L}\right|_{U_M,U_R,U_I,U_x}, \\
\frac{1}{T_M} &= \frac{1}{T'_M} - \left.\frac{\partial S_x}{\partial U_M}\right|_{U_L,U_R,U_I,U_x}, \\
\frac{1}{T_R} &= \frac{1}{T'_R} - \left.\frac{\partial S_x}{\partial U_R}\right|_{U_L,U_M,U_I,U_x}, \\
\frac{1}{T_I} &= \frac{1}{T'_I} - \left.\frac{\partial S_x}{\partial U_I}\right|_{U_L,U_M,U_R,U_x}.
\end{aligned}
\tag{2}
$$

We represent the substrate entropy S_c using the entropies of the separate baths and their correlated entropy S_x,

$$
S_c = S_L + S_M + S_R + S_I - S_x. \tag{3}
$$

Taking the partial derivative of Eq. (3) with respect to the internal energy of the substrate (U_c), we derive Eq. (2). Here, U_P, U_Q, and U_x stand for the expected value of bath P states, bath Q states, and bath P and Q state correlation ($P, Q \in \{L, M, R, I\}$) Hamiltonian, respectively. The terms in Eq. (2), we represent

$$
\frac{1}{T_P} = \left.\frac{\partial S_c}{\partial U_P}\right|_{U_Q,U_x}, \tag{4}
$$

$$
\frac{1}{T'_P} = \left.\frac{\partial S_P}{\partial U_P}\right|_{U_Q,U_x}. \tag{5}
$$

The correlated entropy as in Ref. [36] expresses

$$
\begin{aligned}
S_x &= S(\hat{\rho}_c || \hat{\rho}_L \otimes \hat{\rho}_M \otimes \hat{\rho}_R \otimes \hat{\rho}_I) \\
&= \mathrm{Tr}(\hat{\rho}_c(\ln \hat{\rho}_c - \ln(\hat{\rho}_L \otimes \hat{\rho}_M \otimes \hat{\rho}_R \otimes \hat{\rho}_I)),
\end{aligned}
$$

where

$$
\hat{\rho}_c = \frac{\exp\left(-\frac{H^c_{\mathrm{bath}}}{kBT_c}\right)}{\mathrm{Tr}\left[\exp\left(-\frac{H^c_{\mathrm{bath}}}{kBT_c}\right)\right]},
$$

$$
\hat{\rho}_P = \frac{\exp\left(-\frac{H^P_{\mathrm{bath}}}{kBT'_P}\right)}{\mathrm{Tr}\left[\exp\left(-\frac{H^P_{\mathrm{bath}}}{kBT'_P}\right)\right]}.
$$

We define H^P_{bath} and H^c_{bath} according to Eq. (8).

A. System Hamiltonian

We utilize the system Hamiltonian $\hat{H}^s_{\mathrm{sys}}$ for each transistor according to the previous model [9] as

$$
\begin{aligned}
\hat{H}^s_{\mathrm{sys}} = \frac{\hbar}{2}\big(&\omega^s_L \hat{\sigma}^{s,L}_z + \omega^s_M \hat{\sigma}^{s,M}_z + \omega^s_R \hat{\sigma}^{s,R}_z \\
&+ \omega^s_{LM}\hat{\sigma}^{s,L}_z\hat{\sigma}^{s,M}_z + \omega^s_{MR}\hat{\sigma}^{s,M}_z\hat{\sigma}^{s,R}_z + \omega^s_{RL}\hat{\sigma}^{s,R}_z\hat{\sigma}^{s,L}_z\big),
\end{aligned}
\tag{6}
$$

where $\hbar$ is the reduced Planck constant, $\hbar\omega^s_P$ is the energy difference between the two eigenstates of the TLS P, $\hbar\omega^s_{PQ}$ is the interaction energy between the TLS P and TLS Q ($P, Q \in \{L, M, R\}$), and $\hat{\sigma}_z$ is the 2×2 Pauli matrix. Here, $\hat{\sigma}^{s,P}_z$ are appropriately expanded for each transistor as

$$
\begin{aligned}
\hat{\sigma}^{s,L}_z &= \hat{\sigma}_z \otimes \hat{I} \otimes \hat{I}, \\
\hat{\sigma}^{s,M}_z &= \hat{I} \otimes \hat{\sigma}_z \otimes \hat{I}, \\
\hat{\sigma}^{s,R}_z &= \hat{I} \otimes \hat{I} \otimes \hat{\sigma}_z.
\end{aligned}
\tag{7}
$$

We use identical transistors for ease of analysis. The Hamiltonian of the baths is characterized according to the Caldeira-Leggett model [37], represented by a collection of harmonic oscillators,

$$
\hat{H}^P_{\mathrm{bath}} = \sum_k \hbar\omega^P_k \hat{a}^{P\dagger}_k \hat{a}^P_k. \tag{8}
$$

If we split up the DP, it comprises two individual transistors each formed with three TLSs coupled to three baths at different temperatures as in Fig. 3. The analysis in Secs. IV and V A treats the combined model as two separate transistors. Then, we explain the combined dynamics in Sec. VI C.

III. ENGINEERED INTERACTION HAMILTONIAN TO CREATE QUANTUM CORRELATION

We start with the derivation of the system-bath interaction Hamiltonian. To study possible indirect multiple TLS interactions and direct TLS interactions, we identify a Hamiltonian for a multiatom interaction along the x-direction. The choosing of this direction is due to the possibility of generating a set of desired additional jumps between the energy levels of the system when annihilation and creation operators of the baths acted on them. The possibility for decomposing $\hat{\sigma}_x\hat{\sigma}_x$ terms to $\hat{\sigma}_-\hat{\sigma}_+/\hat{\sigma}_-\hat{\sigma}_-$ will help create energy changes similar to a $\hat{\sigma}_x$ acted on the baths in the composite system. We consider an interaction of three neighboring atoms represented by $j \in \{1, 2\}$. Here, we consider a multisystem introducing $s \in \{1, 2, \ldots, n\}$ to identify a Hamiltonian as

$$
\hat{H}^s_{\mathrm{TLS\text{-}TLS}} = \hbar\omega^s_j\big(V^{s,j,j+1}\sigma^{s,j}_x\sigma^{s,j+1}_x\big), \tag{9}
$$
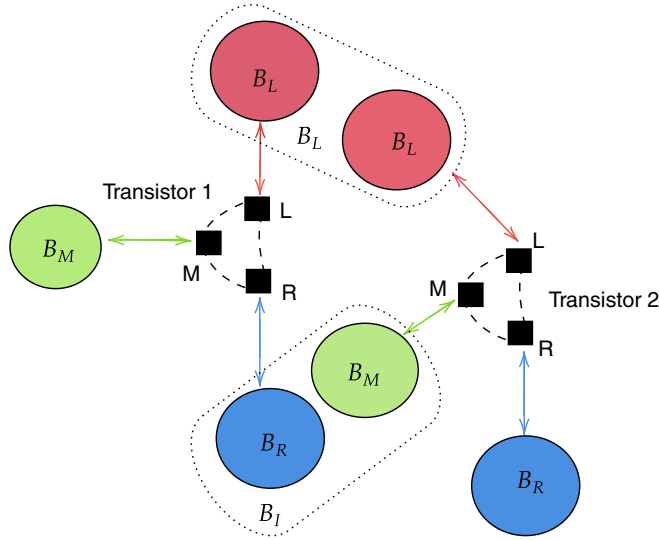
FIG. 3. This illustration provides a visualization of how two individual transistors make a Darlington pair arrangement. Each of the two transistors consists of three TLSs and three baths L, M, and R arranged in a ringlike geometry, thus a TLS is coupled to two neighboring TLSs.

where $V^{s,j,j+1}$ is a coupling constant between two atoms. We approximate the adjacent pair of TLSs joint interaction to the Hamiltonian in Eq. (9), and we define a new Hermitian operator corresponding to the TLS correlations. We use this operator to interpret the TLS joint absorption/emission when it comes in contact with a bath. We represent this Hermitian operator as

$$\hat{S}_x^{s,j,j+1} = V^{s,j,j+1} \hat{\sigma}_x^{s,j} \hat{\sigma}_x^{s,j+1}, \quad (10)$$

where $\hat{S}_x^{s,j,j+1} = (\hat{S}_x^{s,j,j+1})^\dagger$. We then link the energy of two TLSs joint absorption/emission proportionate to ω_j^s to the position of the harmonic oscillators of the bath. This is inspired by Refs. [33] and [39]. Accordingly, when two separate atoms interact with a single-mode resonator, a single photon is directly and jointly absorbed by two atoms. The signal directly emitted from a TLS is proportional to the TLS excitation number, $\langle \hat{C}^- \hat{C}^+ \rangle$. Here, $\hat{C}^-$ and $\hat{C}^+$ are TLS positive and negative frequency operators defined as

$$\hat{C}^+ = \sum_{j,k(k>j)} C_{jk} |j\rangle\langle k|,$$

$$C_{jk} = \langle j|\hat{\sigma}_- + \hat{\sigma}_+|k\rangle,$$

$$\hat{C}^- = (\hat{C}^+)^\dagger.$$

When the mean excitation number for TLS 1 is $\langle \hat{C}_1^- \hat{C}_1^+ \rangle$ and TLS 2 is $\langle \hat{C}_2^- \hat{C}_2^+ \rangle$, the two-TLS correlation stands for

$$G_q = \langle \hat{C}_1^- \hat{C}_2^- \hat{C}_1^+ \hat{C}_2^+ \rangle.$$

According to Ref. [39], the single TLS excitation $\langle \hat{C}_i^- \hat{C}_i^+ \rangle$, where $i \in 1, 2$, and G_q almost coincide at any time, and this two-TLS correlation is an indicator of a joint excitation. Hence, we use this concept to design our interaction Hamiltonian and assume that if one TLS gets excited, the probability that its correlated TLS gets excited is 1.
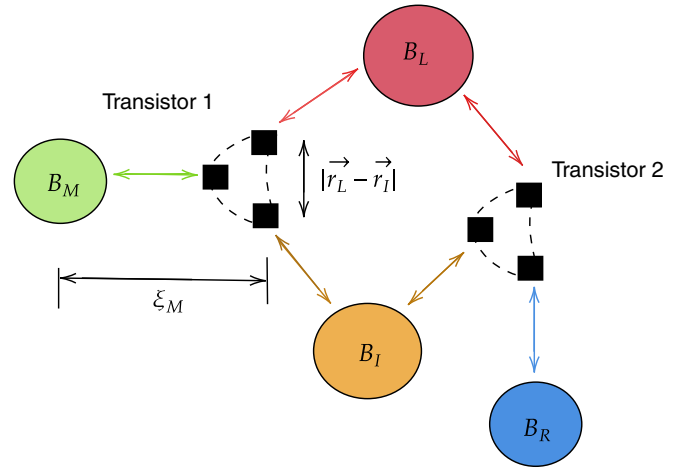
FIG. 4. The diagram shows the spatial distance ξ_P, which is the distance between the system components and individual bath B_P. The distance between an adjacent pair of a directly coupled TLS is $|\mathbf{r}_{P'} - \mathbf{r}_{P''}|$. If $\xi_P \gg |\mathbf{r}_{P'} - \mathbf{r}_{P''}|$, the pair feels the same environmental action, where $P, P', P'' \in \{L, M, I, R\}$. Thus, all three TLSs have couplings to a common environment. Here B_M can be considered a common environment to the transistor 1. Similarly, the separate bath B_R can be a common environment to the transistor 2, and B_L and B_I can be a common environment to both transistors.

Thus, for a bath mode with ω_j^s, it will excite both the TLSs simultaneously.

Next, let us introduce a spatial scale ξ_P that describes the distance between the system components and the bath B_P. This scale depends on system frequency and environment dispersion. Except for the TLS that directly connects to B_P, if the distance between its adjacent pair is $|\mathbf{r}_{P'} - \mathbf{r}_{P''}|$, and this distance satisfies the condition $\xi_P \gg |\mathbf{r}_{P'} - \mathbf{r}_{P''}|$ ($P, P', P'' \in \{L, M, I, R\}$), both the TLSs in the pair will feel the same environmental action [40]. The spatial distance to a pair of TLSs adjacent to the TLS directly coupled to B_M is shown in Fig. 4. If this distance satisfies the condition described, B_M is considered a common environment to the transistor 1. Similarly, the separate bath B_R is a common environment to the transistor 2, and B_L and B_I are a common environment to both transistors. If we consider bath B_P ($P \in \{L, M, I, R\}$) as a common bath, TLSs surrounding it are at different distances. Hence, the direct TLS will feel a different coupling strength than the indirectly interacted TLSs. We assume that the TLS, which is directly coupled to a bath l, has a weak coupling constant $g_k^{s,l}$ while its adjacent pair has a coupling constant

$$f_k^{s,l} = f_l g_k^{s,l}. \quad (11)$$

Here, f_l is a constant, and k represents the modes of the oscillators that comprise the bath. Thus, we assume that the bath interacts with the system operator $\hat{\sigma}_x^{s,j}$ with a weak coupling constant $g_k^{s,l}$, and $\hat{S}_x^{s,j}$ with a weaker but different coupling constant $f_k^{s,l}$. We address these direct/indirect interactions simultaneously in Sec. V, and separately in Sec. VI.

We define the interaction Hamiltonian with k modes for a bath l as

$$\hat{H}^s_{\text{sys-bath}} = \hbar \sum_j^3 \hat{\sigma}^{s,j}_x \sum_k g^{s,l}_k (\hat{a}^{s,l}_k + \hat{a}^{s,l^+}_k) + \hbar \sum_{j=2}^3 \hat{S}^{s,j,j+1}_x \sum_k f^{s,l}_k (\hat{a}^{s,l}_k + \hat{a}^{s,l^+}_k)$$

$$= \hbar \left(\sum_j^3 \hat{\sigma}^{s,j}_x + f_l V^{s,j,j+1} \sum_{j=1}^2 \hat{\sigma}^{s,j}_x \hat{\sigma}^{s,j+1}_x \right) \sum_k g^{s,l}_k (\hat{a}^{s,l}_k + \hat{a}^{s,l^+}_k)$$

$$= \hbar \left(\sum_j^3 \hat{\sigma}^{s,j}_x + \sum_{j=1}^2 f_l V^{s,j,j+1} \hat{\sigma}^{s,j}_x \hat{\sigma}^{s,j+1}_x \right) \sum_k g^{s,l}_k (\hat{a}^{s,l}_k + \hat{a}^{s,l^+}_k). \tag{12}$$

We further expand Eq. (12) considering the TLSs are placed in a ringlike nature as in Fig. 3. Then, we take l as the baths L, M, and R, and j as TLS L, TLS M, and TLS R. Also, $B_{s,l} = \sum_l g^{s,l}_k \sum_k (a^{s,l}_k + a^{\dagger s,l}_k)$. This expansion leads us to define

$$\hat{H}^s_{\text{sys-bath}} = \hbar \big(\hat{\sigma}^{s,L}_x B_{s,L} + \hat{\sigma}^{s,M}_x B_{s,M} + \hat{\sigma}^{s,R}_x B_{s,R} + f_R V^{s,L,M} \hat{\sigma}^{s,L}_x \hat{\sigma}^{s,M}_x B_{s,R} + f_L V^{s,M,R} \hat{\sigma}^{s,M}_x \hat{\sigma}^{s,R}_x B_{s,L} + f_M V^{s,R,L} \hat{\sigma}^{s,R}_x \hat{\sigma}^{s,L}_x B_{s,M} \big), \tag{13}$$

where $\hat{\sigma}^{s,L}_x = \hat{\sigma}_x \otimes I \otimes I$, $\hat{\sigma}^{s,M}_x = I \otimes \hat{\sigma}_x \otimes I$, and $\hat{\sigma}^{s,R}_x = I \otimes I \otimes \hat{\sigma}_x$. Here, $V^{s,m,n}; m, n \in \{L, M, R\}$ represents the dimensionless coupling constant between two correlated TLSs. We define a new term, $\lambda^{mn}_{s,l} = f_l V^{s,m,n}$, which represents a degree of coupling of bath l to the rest of the system represented by correlated TLSs: m and n. We normalize $\lambda^{mn}_{s,l}$ such that $0 \leqslant \lambda^{mn}_{s,l} \leqslant 1$, and we say that when $\lambda^{mn}_{s,l} = 1$, the bath coupling to the rest of the system is complete, and we interpret the pervasive environmental impact. When $\lambda^{mn}_{s,l} = 0$, we say that there is no bath coupling to the rest of the system, and we analyze the system without common environmental effects. Hence, we rewrite Eq. (13) for our model as

$$\hat{H}^s_{\text{sys-bath}} = \hbar \big(\underbrace{\hat{\sigma}^{s,L}_x B_{s,L}}_{\text{TLS-bath}} + \underbrace{\hat{\sigma}^{s,M}_x B_{s,M}}_{\text{TLS-bath}} + \underbrace{\hat{\sigma}^{s,R}_x B_{s,R}}_{\text{TLS-bath}} + \lambda^{LM}_{s,R} \underbrace{\hat{\sigma}^{s,L}_x \hat{\sigma}^{s,M}_x}_{\text{TLS-TLS}} \underbrace{B_{s,R}}_{\text{correlated TLS-bath}} + \lambda^{MR}_{s,L} \underbrace{\hat{\sigma}^{s,M}_x \hat{\sigma}^{s,R}_x}_{\text{TLS-TLS}} \underbrace{B_{s,L}}_{\text{correlated TLS-bath}} + \lambda^{RL}_{s,M} \underbrace{\hat{\sigma}^{s,R}_x \hat{\sigma}^{s,L}_x}_{\text{TLS-TLS}} \underbrace{B_{s,M}}_{\text{correlated TLS-bath}} \big),$$

which further simplifies as the interaction Hamiltonian of bath P to rest of the system

$$\hat{H}^{s,P}_{\text{sys-bath}} = \hbar \big(\hat{\sigma}^{s,P}_x + \lambda^{QR}_{s,P} \hat{\sigma}^{s,Q}_x \hat{\sigma}^{s,R}_x \big) \sum_k g^{s,P}_k \big(\hat{a}^{s,P}_k + \hat{a}^{s,P \dagger}_k \big), \tag{14}$$

where $P, Q, R \in \{L, M, R\}$. In addition, k defines the thermal bath modes, $\hat{a}^P_k$ and $\hat{a}^{\dagger P}_k$ represent the annihilation and creation operators on the bath mode with frequency ω^P_k, and g^P_k represents the coupling strength between the kth bath mode and the appropriate TLS. These thermal interactions change the quantum states of the directly coupled TLS as well as its adjacent pair, represented by Q and R with a probability $\lambda^{QR}_{s,P}$. Here, $\lambda^{QR}_{s,P}$ is the degree of coupling of the reservoir P to the rest of the system [33]. Note that we can represent $\hat{\sigma}_x = \hat{\sigma}_+ + \hat{\sigma}_-$. Hence, we further expand Eq. (14) as

$$\hat{H}^s_{\text{sys-bath}} = \hbar \big(\hat{\sigma}^{s,L}_- + \lambda^{MR}_{s,L} \hat{\sigma}^{s,M}_+ \hat{\sigma}^{s,R}_- + \lambda^{MR}_{s,L} \hat{\sigma}^{s,M}_- \hat{\sigma}^{s,R}_- \big) B_{s,L} + \hbar \big(\hat{\sigma}^{s,M}_- + \lambda^{RL}_{s,M} \hat{\sigma}^{s,R}_+ \hat{\sigma}^{s,L}_- + \lambda^{RL}_{s,M} \hat{\sigma}^{s,R}_- \hat{\sigma}^{s,L}_- \big) B_{s,M}$$

$$+ \hbar \big(\hat{\sigma}^{s,R}_- + \lambda^{LM}_{s,R} \hat{\sigma}^{s,L}_+ \hat{\sigma}^{s,M}_- + \lambda^{LM}_{s,R} \hat{\sigma}^{s,L}_- \hat{\sigma}^{s,M}_- \big) B_{s,R} + \text{H.c.}, \tag{15}$$

where H.c. is the Hermitian conjugate. For our design, we assume that we can use reservoir engineering to restrict some of the interactions, and we create additional channels of dissipation that were not present in the original design in Ref. [9]. A close analysis of this interaction Hamiltonian shows that a reservoir can flip a single-spin as well as a double-spin flip in the system as in Fig. 5. A single-spin transition corresponds to a state change where there is only one spin change, whereas a double-spin transition corresponds to two possible spin changes. The simultaneous transition of these single- and double-spin flips due to a single excitation in the environment can happen in our model when angular frequencies of the TLSs satisfy $\omega^s_L = \omega^s_M = \omega^s_R = \omega^s_{RL} = 0$, and $\omega^s_{MR} > \omega^s_{LM} > 0$. When the angular frequencies satisfy $\omega^s_L = \omega^s_M - \omega^s_R$, the transitions between the energy levels happen according to Fig. 6. We restrict most of these interactions and select only the double-spin flip transitions happening in the same energy as the single-spin flip transitions. Hence, we select only the necessary terms from Eq. (15), and we express our interaction Hamiltonian as

$$\hat{H}^s_{\text{sys-bath}} = \hbar \big[\big(\hat{\sigma}^{s,L}_- + \lambda^{MR}_{s,L} \hat{\sigma}^{s,M}_+ \hat{\sigma}^{s,R}_- \big) B_{s,L} + \big(\hat{\sigma}^{s,M}_- + \lambda^{RL}_{s,M} \hat{\sigma}^{s,R}_- \hat{\sigma}^{s,L}_- \big) B_{s,M} + \big(\hat{\sigma}^{s,R}_- + \lambda^{LM}_{s,R} \hat{\sigma}^{s,L}_- \hat{\sigma}^{s,M}_+ \big) B_{s,R} \big]. \tag{16}$$

For example, carefully analyzing Eq. (16), we can see that a boson in the bath with energy $E_L = \hbar \omega_L$ can induce a single-spin flip through operators $\hat{a}^{+s,L}_k \hat{\sigma}^{s,L}_-$ as well as a double-spin flip through $\hat{a}^{+s,L}_k \hat{\sigma}^{s,M}_+ \hat{\sigma}^{s,R}_-$ with a probability $\lambda^{MR}_{s,L}$. The

correlated TLS terms and the reservoir engineering in the TLS-bath interactions create quantum entanglement. Quantum entanglement captures the quantum correlation between two quantum systems. We deduce the system jump operators
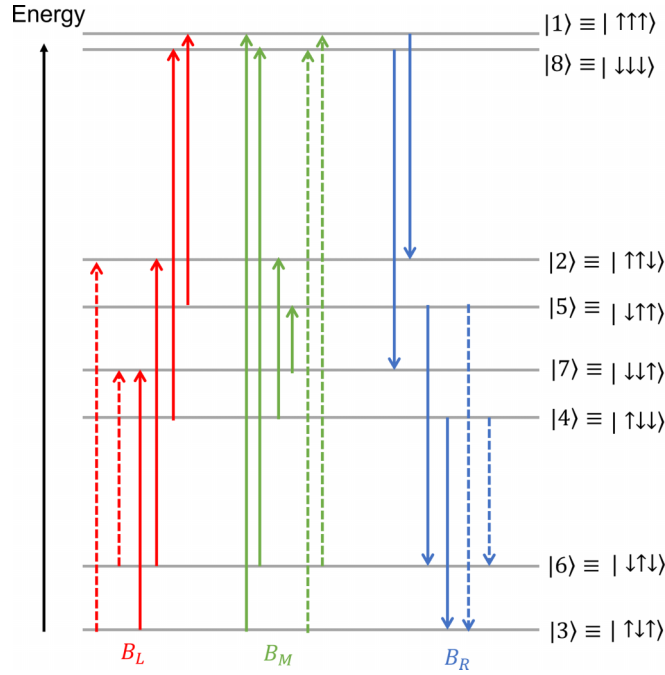
FIG. 5. Single-spin flip transitions (transitions from one state to the other where the differences in the two states are by a single-spin change, and spins are represented by arrows $\uparrow, \downarrow$) caused by direct interactions with baths B_L, B_M, and B_R in the system are shown by solid lines. The double-spin flip transitions (transitions from one state to the other where the differences in the two states are by two spin changes) are induced due to indirect interactions with baths B_L, B_M, and B_R and are shown by dashed lines. This follows the interaction Hamiltonian in Eq. (16). The thermal flow through the device happens via these transitions. Transitions induced by B_L (including the dashed lines) drive a portion of ground states $|3\rangle$ and $|6\rangle$ populations to $|2\rangle$ and $|7\rangle$. The populations established in $|4\rangle$ and $|5\rangle$ are sent back to ground states $|3\rangle$ and $|6\rangle$ (even by dashed lines) by B_R. The extra energy required to make the jump from $|2\rangle$ to $|4\rangle$ and $|7\rangle$ to $|5\rangle$ is provided by thermal bath B_M. This type of energy level diagram describes a composite system with not-in resonant two-level systems. We use this diagram to represent our incoherent-correlated model.

from Eq. (16) as

$$\hat{A}_L^s = \hat{\sigma}_L^{s-} + \lambda_{s,L}^{MR}\hat{\sigma}_M^{s+}\hat{\sigma}_R^{s-},$$
$$\hat{A}_M^s = \hat{\sigma}_M^{s-} + \lambda_{s,M}^{RL}\hat{\sigma}_R^{s-}\hat{\sigma}_L^{s-},$$
$$\hat{A}_R^s = \hat{\sigma}_R^{s-} + \lambda_{s,R}^{LM}\hat{\sigma}_L^{s-}\hat{\sigma}_M^{s+}. \tag{17}$$

Then, we perform spectral decomposition on the jump operators. In the eigendecomposition of the system Hamiltonian $\hat{H}_{\text{sys}}^s = \sum_i \epsilon_i |\epsilon_i\rangle\langle\epsilon_i|$, the spectral decomposition of the jump operators in Eq. (17) leads to

$$\hat{A}_L^s(\omega) = \sum_{\epsilon'-\epsilon=\hbar\omega} |\epsilon\rangle\langle\epsilon|\hat{A}_L^s|\epsilon'\rangle\langle\epsilon'|,$$

$$\hat{A}_M^s(\omega) = \sum_{\epsilon'-\epsilon=\hbar\omega} |\epsilon\rangle\langle\epsilon|\hat{A}_M^s|\epsilon'\rangle\langle\epsilon'|,$$

$$\hat{A}_R^s(\omega) = \sum_{\epsilon'-\epsilon=\hbar\omega} |\epsilon\rangle\langle\epsilon|\hat{A}_R^s|\epsilon'\rangle\langle\epsilon'|, \tag{18}$$

where $\epsilon' > \epsilon$, and the operators satisfy

$$\sum_\omega \hat{A}_P^s(\omega) = \sum_\omega \hat{A}_P^{\dagger s}(\omega) = \hat{A}_P^s,$$
$$[\hat{H}_{\text{sys}}, \hat{A}_P^s(\omega)] = \omega\hat{A}_P^s(\omega),$$
$$[\hat{H}_{\text{sys}}, \hat{A}_P^s(-\omega)] = -\omega\hat{A}_P^s(\omega).$$

In the incoherent-correlated model, we assume that the single-spin flip and double-spin flip transitions happen independently and not simultaneously corresponding to the different frequencies of the bath modes. Figures 5 and 6 show the energy diagram with the possible relaxations for a transistor in the DP. While solid arrows show the transitions that were in the previous model [9], the dashed arrows indicate the additional channels achieved via reservoir engineering. For our incoherent-correlated model, we represent the decomposed jump operators as

$$\hat{A}_{L1}^s(\omega) = \sum_{\epsilon'-\epsilon=\hbar\omega} |\epsilon\rangle\langle\epsilon|\hat{\sigma}_L^{s-}|\epsilon'\rangle\langle\epsilon'|,$$

$$\hat{A}_{L2}^s(\omega) = \sum_{\epsilon'-\epsilon=\hbar\omega} |\epsilon\rangle\langle\epsilon|\lambda_L^{MR}\hat{\sigma}_M^{s+}\hat{\sigma}_R^{s-}|\epsilon'\rangle\langle\epsilon'|,$$

$$\hat{A}_{M1}^s(\omega) = \sum_{\epsilon'-\epsilon=\hbar\omega} |\epsilon\rangle\langle\epsilon|\hat{\sigma}_M^{s-}|\epsilon'\rangle\langle\epsilon'|,$$

$$\hat{A}_{M2}^s(\omega) = \sum_{\epsilon'-\epsilon=\hbar\omega} |\epsilon\rangle\langle\epsilon|\lambda_M^{RL}\hat{\sigma}_R^{s-}\hat{\sigma}_L^{s-}|\epsilon'\rangle\langle\epsilon'|,$$

$$\hat{A}_{R1}^s(\omega) = \sum_{\epsilon'-\epsilon=\hbar\omega} |\epsilon\rangle\langle\epsilon|\hat{\sigma}_R^{s-}|\epsilon'\rangle\langle\epsilon'|,$$

$$\hat{A}_{R2}^s(\omega) = \sum_{\epsilon'-\epsilon=\hbar\omega} |\epsilon\rangle\langle\epsilon|\lambda_R^{LM}\hat{\sigma}_L^{s-}\hat{\sigma}_M^{s+}|\epsilon'\rangle\langle\epsilon'|. \tag{19}$$
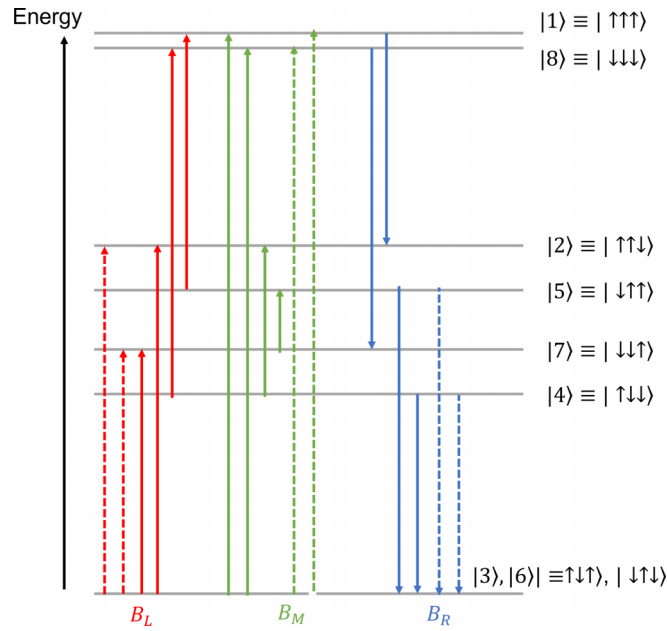
FIG. 6. Single-spin flip transitions (transitions from one state to the other where the differences in the two states are by a single-spin change, and spins are represented by arrows $\uparrow, \downarrow$), and double-spin flip transitions (transitions from one state to the other where the differences in the two states are by two spin changes) are caused by engineered interactions with baths B_L, B_M, and B_R when the two ground states $|3\rangle$ and $|6\rangle$ are degenerate. This is represented by solid lines and dashed lines, respectively. Due to the degeneracy, we can configure angular frequencies to make the single-spin flip and double-spin flip transitions: $|3\rangle, |6\rangle \to |2\rangle, |7\rangle$ induced by B_L; $|3\rangle, |6\rangle \to |1\rangle, |8\rangle$ induced by B_M; $|5\rangle, |4\rangle \to |3\rangle, |6\rangle$ induced by B_R; to have the same energy. This type of energy level diagram describes a composite system with resonant two-level systems where their energies satisfy $\hbar\omega_M^s - \hbar\omega_L^s = \hbar\omega_R^s$. We use this diagram to represent our incoherent-correlated model tuned to contain a dark-state.

In an individual transistor system, there are 28 different possible jumps from $|\epsilon'\rangle$ to $|\epsilon\rangle$, however only 18 of them are nonzero.

The thermal flows through the device happen due to the transitions induced by the thermal baths. At the steady state, the ground states are more populated than the highest energy states. Hence, we neglect some of the transitions between higher energy levels (e.g., from $|1\rangle$ and $|8\rangle$) and transitions with high energy gaps (e.g., $|3\rangle - |8\rangle$, $|6\rangle - |1\rangle$). Transitions induced by B_L (including the double dot transition lines) drive a portion of ground states $|3\rangle$ and $|6\rangle$ populations to $|2\rangle$ and $|7\rangle$. The populations established in $|4\rangle$ and $|5\rangle$ are sent back to the ground states $|3\rangle$ and $|6\rangle$ (even by dashed lines) induced from B_R. The extra energy required to make the jump from $|2\rangle$ to $|4\rangle$ and $|7\rangle$ to $|5\rangle$ is provided by the thermal bath B_M. If T_M is too low, B_M cannot provide the necessary energy for this jump. Hence, there will not be a thermal flow from B_L to B_R. Our analysis shows that double-spin flip transitions can be engineered to help drive the transitions from the ground states to higher states.

If we do not make restrictions to other indirect bath interactions, there will be additional relaxations as in Fig. 7. Here, one of the key relaxations of B_M is between $|5\rangle$ to $|2\rangle$ and $|7\rangle$ to $|4\rangle$. If one of these happens, it can disturb the maintenance of populations for the system at the desired ratio when driving populations from $|2\rangle$ to $|4\rangle$ and $|7\rangle$ to $|5\rangle$. This disrupts the stability of the system. Hence, we restrict such interactions intentionally by selecting the interaction Hamiltonian as in Eq. (16).

IV. FORMALISM

The total Hamiltonian $\hat{H}^s$ of the transistor and its environment now reads

$$\hat{H}^s = \hat{H}_{\text{sys}}^s + \sum_{P \in \{L,M,R\}} \left(\hat{H}_{\text{bath}}^P + \hat{H}_{\text{sys-bath}}^P \right). \quad (20)$$

We switch to the interaction picture and solve our model defined by the total Hamiltonian $\hat{H}^s$. We use a local approach and neglect the weak inter-TLS interaction Hamiltonian when deriving the master equation as in Refs. [38,41,42]. Our Hamiltonian is already diagonalized in the bare states, and the populations depend on the dissipative dynamics only. At the steady state, all coherence terms in the density matrix reach zero (see Appendix A for the derivation of the quantum master equation [33,43–45]). We represent our master equation for the composite system under the weak coupling regime for n number of individual transistors as

$$\frac{d\hat{\rho}(t)}{dt} = \sum_{s \in \{1,2,\ldots,n\}} \sum_{P \in \{L,M,R\}} \mathcal{L}_P^s[\hat{\rho}^s(t)] \quad (21)$$

in the interaction picture. In our formalism, we treat the multitransistor model as a collection of individual systems represented by s. Hence, the master equation for an individual system is given by

$$\frac{d\hat{\rho}^s(t)}{dt} = \sum_{P \in \{L,M,R\}} \mathcal{L}_P^s[\hat{\rho}^s(t)]. \quad (22)$$
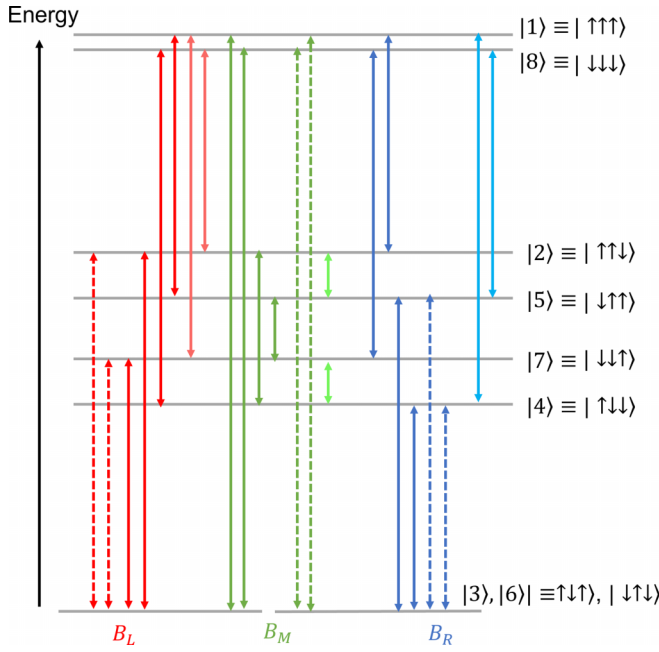
FIG. 7. Without any restrictions, single-spin flip transitions (transitions from one state to the other where the differences in the two states are by a single-spin change, and spins are represented by arrows $\uparrow$, $\downarrow$) and double-spin flip transitions (transitions from one state to the other where the differences in the two states are by two spin changes) are caused by the interactions with bath B_L, B_M, and B_R. These transitions are marked as solid lines and dashed lines, respectively. The additional transitions are also included using solid lines. One of the key relaxations from B_M between $|5\rangle$–$|2\rangle$ and $|7\rangle$–$|4\rangle$ must be avoided to maintain the stability of the transistor. This energy level diagram provides us with all the possible transitions of an incoherent model without engineered reservoir interactions.

We assume that even under the common environment interactions, the system bath couplings remain weak so that we can safely apply rotating wave approximations (RWAs). We obtain the Lindblad terms as in Eq. (23),

$$
\begin{aligned}
\mathcal{L}_P^s[\hat{\rho}^s] = \sum_{\omega>0}\bigg[& \mathcal{J}_P^s(\omega)[1+n_P^s(\omega)]\bigg(\hat{A}_P^s(\omega)\hat{\rho}^s\hat{A}_P^{s\dagger}(\omega) \\
& -\frac{1}{2}\big\{\hat{A}_P^{s\dagger}(\omega)\hat{A}_P^s(\omega),\hat{\rho}^s\big\}\bigg)+\mathcal{J}_P^s(\omega)n_P^s(\omega) \\
& \times\bigg(\hat{A}_P^{s\dagger}(\omega)\hat{\rho}^s\hat{A}_P^s(\omega)-\frac{1}{2}\big\{\hat{A}_P^s(\omega)\hat{A}_P^{s\dagger}(\omega),\hat{\rho}^s\big\}\bigg)\bigg],
\end{aligned}
$$
(23)

where $P \in \{L, M, R\}$. In Eq. (23), ω runs through all allowed 28 positive energy transitions of each of the individual eight-level quantum system. However, the Lindblad terms are only nonzero for the energies where there is a transition from one state to the other. The individual thermal bath temperature for each transistor T_P^s influences the dynamics of the whole system through

$$
n_P^s(\omega) = \frac{1}{\exp\left(\frac{\hbar\omega}{k_B T_P^s}\right)-1},
$$
(24)

where k_B is the Boltzmann constant. Assuming the baths to be Ohmic, we describe the spectral density function $\mathcal{J}_P^s(\omega)$. Here, ω_{LD} stands for the Lorentz-Drude cutoff frequency,

$$
\mathcal{J}_P^s(\omega) = \kappa_P^s\omega\frac{\omega_{LD}^2}{\omega_{LD}^2+\omega^2}.
$$
(25)

Assuming the frequencies of the individual transistors are much smaller than ω_{LD}, we define the spectral density function as

$$
\mathcal{J}_P^s(\omega) = \kappa_P^s\omega,
$$
(26)

where κ_P^s describes the modulation of the thermal bath's direct influence on the dynamics of the quantum transistor s.

Note that, for a given temperature T_P and frequency between two energy levels $\omega_{j,k}$, the populations in the density matrix satisfy the ratio at which the thermal baths balance their state populations given by

$$
\frac{\rho_{jj}}{\rho_{kk}} = \frac{n_P(\omega_{jk})}{1+n_P(\omega_{jk})}.
$$
(27)

V. QUANTUM CORRELATION AND EMERGENCE OF QUANTUM ENTANGLEMENT

Quantum entanglement can happen as a consequence of quantum correlation when multiple components of the system interact with the environment simultaneously [24]. Allowing simultaneous single-spin flip and double-spin flip transitions, it is possible to preserve quantum coherence. In the literature, this is achieved through a dark-state. We provide an analysis on how the system dynamics change and how this affects the heat flows when we allow such simultaneous transitions. We show that it is possible to tune our system to contain a dark-state that is the entanglement of the two ground states of our system.

A. Formation of dark-states

In general, a dark-state is a superposition of two lowest states without dipole transitions between them [26]. The presence of a dark-state can be regarded as a method of preserving quantum coherence [32]. In specific configurations, system environment couplings can be used to engineer a dark-state via quantum entanglement [46].

Liu *et al.* [34] showed that heat currents through a thermal transistor at a steady state depend on the initial state of a dark-state given appropriate parameters. Further, they demonstrated that in the case of completely correlated transitions, the transistor can be provided with an external channel to control the heat currents, but this does not affect the amplification rate. Inspired by this work, we show the possibility of tuning our DP model to two dark-states and the likelihood of creating additional applications with the use of other multitransistor configurations.

B. Tuning the two-transistor model to contain dark-states

This section analyzes how to tune a two-transistor model to contain dark-states. We select the jump operators as in Eq. (17). Then we set $\lambda_{s,P}^{QR} = 1$ and choose the angular frequency parameters such that the two sets of three TLSs are

in resonance. Hence, the three TLSs on each transistor satisfy $\omega_M^s - \omega_L^s = \omega_R^s$. This constraint creates two degenerate ground states $|3\rangle^s$ and $|6\rangle^s$ ($s \in \{1, 2\}$) for each transistor as in Fig. 6. If $\omega_M^s = \omega_L^s = \omega_R^s = 0$ and $\omega_{MR}^s > \omega_{LM}^s > 0$, all the relaxations between the ground states and the excited states become equal in energy. This condition helps tune the transistor to a dark-state. By appropriate reservoir interactions, it is possible to create a dark-state $|-\rangle^s$ and a bright-state $|+\rangle^s$, respectively, of the form

$$|-\rangle^s = \sin\theta|3\rangle^s - \cos\theta|6\rangle^s,$$
$$|+\rangle^s = \sin\theta|3\rangle^s + \cos\theta|6\rangle^s,$$

using quantum entanglement [32]. Here, θ is the angle between the two degenerate states. We ultimately find θ by solving the transistor dynamics using the Lindblad terms in Eq. (28). Here, we assume that all the transitions induced by the Pth bath happen with the same energy and same transition rate. Bath P will couple to the single TLS P as well as to the other transitions with energy $E_P^s = \hbar\omega_P^s$. Thus, we take the angular frequencies of the TLSs as $\omega_M^s = \omega_L^s = \omega_R^s = \omega_{RL} = 0$ and $\omega_{MR}^s > \omega_{LM}^s > 0$. Therefore, Eq. (28) is Eq. (23) with only one energy change per bath given by

$$\mathcal{L}_P^s[\hat{\rho}^s] = \mathcal{J}_P^s(\omega_P)[1 + n_P^s(\omega_P)]\left(\hat{A}_P^s(\omega_P)\hat{\rho}^s\hat{A}_P^{s\dagger}(\omega_P)\right.$$
$$- \frac{1}{2}\{\hat{A}_P^{s\dagger}(\omega_P)\hat{A}_P^s(\omega_P), \hat{\rho}^s\}\right) + \mathcal{J}_P^s(\omega_P)n_P^s(\omega_P)$$
$$\times \left(\hat{A}_P^{s\dagger}(\omega_P)\hat{\rho}^s\hat{A}_P^s(\omega_p) - \frac{1}{2}\{\hat{A}_P^s(\omega_P)\hat{A}_P^{s\dagger}(\omega_P), \hat{\rho}^s\}\right).$$
$$(28)$$

When we solve each of the Lindblad terms, we see the formation of a new state under $|3\rangle^s$ and $|6\rangle^s$ having equal probability of populations. At a steady state, the new state and its conjugate can be described as

$$\rho_{++}^s = \frac{1}{2}(\rho_{33}^s + \rho_{66}^s + \rho_{36}^s + \rho_{63}^s),$$
$$\rho_{--}^s = \frac{1}{2}(\rho_{33}^s + \rho_{66}^s - \rho_{36}^s - \rho_{63}^s). \qquad (29)$$

Let us call these the bright-state and the dark-state populations, respectively. These state populations comprise populations of ground states (probability of occurrence of each energy level in a particular state) and their coherence between row-state and column-state, represented by ρ_{33}^s, ρ_{66}^s, ρ_{36}^s, and ρ_{63}^s. This result is guaranteed by degenerate $|3\rangle^s$ and $|6\rangle^s$ and the same transition rates to the excited states. Further, it is possible to represent the bright-state and the dark-state for each transistor as

$$|+\rangle^s = \frac{1}{\sqrt{2}}(|3\rangle^s + |6\rangle^s),$$
$$|-\rangle^s = \frac{1}{\sqrt{2}}(|3\rangle^s - |6\rangle^s). \qquad (30)$$

We derive the dynamics of the system density matrix populations as

$$\dot{\rho}_{11}^s = \Gamma_{51}^{s,L} + 2\Gamma_{+1}^{s,M} + \Gamma_{21}^{s,R},$$
$$\dot{\rho}_{22}^s = \Gamma_{42}^{s,M} - \Gamma_{21}^{s,R} + 2\Gamma_{+2}^{s,L},$$
$$\dot{\rho}_{++}^s = 2(\Gamma_{7+}^{s,L} - \Gamma_{+1}^{s,M} + \Gamma_{4+}^{s,R} - \Gamma_{+2}^{s,L} + \Gamma_{8+}^{s,M} - \Gamma_{+5}^{s,R}),$$

$$\dot{\rho}_{44}^s = \Gamma_{84}^{s,L} - \Gamma_{42}^{s,M} - 2\Gamma_{4+}^{s,R},$$
$$\dot{\rho}_{55}^s = -\Gamma_{51}^{s,L} + \Gamma_{75}^{s,M} - 2\Gamma_{5+}^{s,R},$$
$$\dot{\rho}_{--}^s = 0,$$
$$\dot{\rho}_{77}^s = -2\Gamma_{7+}^{s,L} - \Gamma_{75}^{s,M} + \Gamma_{87}^{s,R},$$
$$\dot{\rho}_{88}^s = -\Gamma_{84}^{s,L} - \Gamma_{87}^{s,R} - 2\Gamma_{8+}^{s,M}, \qquad (31)$$

where

$$\Gamma_{jk}^{s,P} = \mathcal{J}_P^s(\omega_P)\left([1 + n_P(\omega_P)]\rho_{jj}^S - n_P(\omega_P)\rho_{kk}^s\right).$$

In this model, we see that $\dot{\rho}_{--}^s = 0$. This implies that there will not be any relaxations to other excited states from $|-\rangle^s$ and will remain with the same probability as in the initial state. Solving these differential equations, we see that the dark-state populations are given by $\rho_{--}^s = \rho_{--}^s(0)$. We also arrive at a proportionality where the transistor steady states are spanned by the initial populations of the dark-state,

$$\rho_{\text{pp}}^s \propto [1 - \rho_{--}^s(0)]; \quad p \in \{1, 2, +, 4, 5, 7, 8\}. \qquad (32)$$

As $\rho_{--}^s(t)$ does not evolve with time, its population remains in the initial state and obeys the probability law

$$\rho_{11}^s + \rho_{22}^s + \rho_{++}^s + \rho_{44}^s + \rho_{55}^s + \rho_{77}^s + \rho_{88}^s = 1 - \rho_{--}^s(0)$$
$$(33)$$

at the steady state. This initial state dependency is similar to that in Refs. [32,34], and it allows us to use an external control like a laser field to control the transistor. For a dark-state to exist, $|3\rangle^s$ and $|6\rangle^s$ have to be degenerate and should be the lowest energy levels that allow single-spin/double-spin transitions to the excited states. Furthermore, the system should satisfy the resonance conditions $\omega_M^s - \omega_L^s = \omega_R^s$. The simultaneous transitions of single-spin flip and double-spin flips create quantum coherence ρ_{36}^s and ρ_{63}^s at the steady state. A careful mapping through derivations shows that a similar condition to switch transistors using a dark-state is possible for an incoherent model even when $\rho_{36}^s = \rho_{63}^s = 0$.

C. Energy flow rates at a coherent correlated dissipation

We can find the energy flow rates to and from the reservoirs to the quantum system by employing the energy conservation principle. Considering the transistors 1 and 2 to be separate, we derive thermal flow rates using

$$\sum_{P \in \{L,M,R\}} J_P^s(t) = \frac{\partial\langle\hat{H}_{\text{sys}}^s\rangle}{\partial t} = \text{Tr}\left\{\hat{H}_{\text{sys}}\frac{d\hat{\rho}^s(t)}{dt}\right\}, \qquad (34)$$

where J_P^s denotes the net energy inflows into the system from the Pth thermal bath. In the coherent correlated model, the energy flow rates appear to show quantum coherence. Using Eq. (34) and the Lindblad terms in Eq. (23), we obtain the separate energy flow rates for the transistor 1 and transistor 2 as in Eq. (35),

$$J_L^s = -\left(\epsilon_{51}^s\Gamma_{51}^{s,L} + 2\epsilon_{7+}^s\Gamma_{7+}^{s,L} + \epsilon_{84}^s\Gamma_{84}^{s,L} + 2\epsilon_{+2}^s\Gamma_{+2}^{s,L}\right),$$
$$J_M^s = -\left(2\epsilon_{+1}^s\Gamma_{+1}^{s,M} + \epsilon_{42}^s\Gamma_{42}^{s,M} + \epsilon_{75}^s\Gamma_{75}^{s,M} + +2\epsilon_{8+}^s\Gamma_{8+}^{s,L}\right.$$
$$\left. + 2\epsilon_{+1}^s\Gamma_{+1}^{s,L}\right),$$
$$J_R^s = -\left(\epsilon_{21}^s\Gamma_{21}^{s,R} + 2\epsilon_{4+}^s\Gamma_{4+}^{s,R} + \epsilon_{87}^s\Gamma_{87}^{s,R} + \epsilon_{5+}^s\Gamma_{5+}^{s,L}\right), \qquad (35)$$

where the energy level difference between the eigenstates represents

$$\epsilon_{+l} = \frac{\epsilon_3 + \epsilon_6}{2} - \epsilon_l,$$

$$\epsilon_{l+} = \epsilon_l - \frac{\epsilon_3 + \epsilon_6}{2}.$$

Here, l corresponds to a state other than the bright-state and the dark-state ($l \in 1, 2, 4, 5, 7, 8$). For a description of the states, refer to Fig. 5. Then, the combined energy flows for the DP model can be obtained using Eq. (42).

VI. INCOHERENT CORRELATED DISSIPATION

The main aim of this paper is to produce a generalized model that can interpret the common environmental effects on the system by treating the common baths as separate baths. This model must also treat the single-spin flip and double-spin flip transitions independently. Therefore, we introduce an incoherent-correlated model named in Ref. [33] for a quantum thermal refrigerator to our multitransistor model. The incoherent term implies that at the steady state there are no coherences in the density matrix. Correlation means that the thermal baths in the environment interact with multiple components in the system and not just the TLS that is directly coupled to them. We explained the formation of quantum correlation through engineered reservoir interactions in Sec. III. Once we assume that the single-spin flip transitions happen independently from the ones achieving paired spin transitions, the transitions can happen either as in Fig. 5 or as in Fig. 6. The difference in Fig. 6 is that the two ground states are degenerate. This occurs under the assumption of resonance conditions. We derive the Lindblad terms using Eq. (23) for the jump operators given in Eq. (19). Thus, we obtain the transistor dynamics for the incoherent-correlated model as

$$\dot{\rho}_{11}^s = + \Gamma_{51}^{s,L} + \Gamma_{31}^{s,M} + \Gamma_{21}^{s,R} + \left(\lambda_{s,M}^{RL}\right)^2 \Gamma_{61}^{s,M},$$

$$\dot{\rho}_{22}^s = + \Gamma_{62}^{s,L} + \Gamma_{42}^{s,M} - \Gamma_{21}^{s,R} + \left(\lambda_{s,L}^{MR}\right)^2 \Gamma_{32}^{s,L},$$

$$\dot{\rho}_{33}^s = + \Gamma_{73}^{s,L} - \Gamma_{31}^{s,M} + \Gamma_{43}^{s,R} - \left(\lambda_{s,L}^{MR}\right)^2 \Gamma_{32}^{s,L}$$
$$+ \left(\lambda_{s,M}^{RL}\right)^2 \Gamma_{83}^{s,M} + \left(\lambda_{s,R}^{LM}\right)^2 \Gamma_{53}^{s,R},$$

$$\dot{\rho}_{44}^s = + \Gamma_{84}^{s,L} - \Gamma_{42}^{s,M} - \Gamma_{43}^{s,R} + \left(\lambda_{s,R}^{LM}\right)^2 \Gamma_{64}^{s,R},$$

$$\dot{\rho}_{55}^s = - \Gamma_{51}^{s,L} + \Gamma_{75}^{s,M} + \Gamma_{65}^{s,R} - \left(\lambda_{s,R}^{LM}\right)^2 \Gamma_{53}^{s,R},$$

$$\dot{\rho}_{66}^s = - \Gamma_{62}^{s,L} + \Gamma_{86}^{s,M} - \Gamma_{65}^{s,R} + \left(\lambda_{s,L}^{MR}\right)^2 \Gamma_{67}^{s,L}$$
$$- \left(\lambda_{s,M}^{RL}\right)^2 \Gamma_{61}^{s,M} - \left(\lambda_{s,R}^{LM}\right)^2 \Gamma_{64}^{s,R},$$

$$\dot{\rho}_{77}^s = - \Gamma_{73}^{s,L} - \Gamma_{75}^{s,M} + \Gamma_{87}^{s,R} - \left(\lambda_{s,L}^{MR}\right)^2 \Gamma_{67}^{s,L},$$

$$\dot{\rho}_{88}^s = - \Gamma_{84}^{s,L} - \Gamma_{86}^{s,M} - \Gamma_{87}^{s,R} - \left(\lambda_{s,M}^{RL}\right)^2 \Gamma_{83}^{s,M}, \quad (36)$$

where

$$\Gamma_{jk}^{s,P} = \mathcal{J}_P^s(\omega_{jk}^s)\left([1 + n_P(\omega_{jk}^s)]\rho_{jj}^S - n_P(\omega_{jk}^s)\rho_{kk}^s\right),$$

which represents the transition rate from state $|j\rangle^s$ to state $|k\rangle^s$ induced by the system-bath thermal interactions. Compared with the previous multitransistor model in Ref. [9], the transistor dynamics now show additional dissipative terms proportionate to $(\lambda_{s,P}^{QR})^2$.

A. Energy flow rates at incoherent correlation dissipation

Using Eq. (34), we find the individual heat flows for transistors 1 and 2 in the incoherent-correlated model. Then, we establish the equivalent energy flow rates for the DP using Eq. (42). In Eq. (37), we represent the individual heat outflow from each bath as

$$J_L^s = - \left(\epsilon_{51}^s \Gamma_{51}^{s,L} + \epsilon_{62}^s \Gamma_{62}^{s,L} + \epsilon_{73}^s \Gamma_{73}^{s,L} + \epsilon_{84}^s \Gamma_{84}^{s,L}\right)$$
$$- \lambda_{s,L}^{MR}\left(\epsilon_{32}^s \Gamma_{32}^{s,L} + \epsilon_{76}^s \Gamma_{76}^{s,L}\right),$$

$$J_M^s = - \left(\epsilon_{31}^s \Gamma_{31}^{s,M} + \epsilon_{42}^s \Gamma_{42}^{s,M} + \epsilon_{75}^s \Gamma_{75}^{s,M} + \epsilon_{86}^s \Gamma_{86}^{s,M}\right)$$
$$- \lambda_{s,M}^{RL}\left(\epsilon_{83}^s \Gamma_{83}^{s,L} + \epsilon_{61}^s \Gamma_{61}^{s,L}\right),$$

$$J_R^s = - \left(\epsilon_{21}^s \Gamma_{21}^{s,R} + \epsilon_{43}^s \Gamma_{43}^{s,R} + \epsilon_{65}^s \Gamma_{65}^{s,R} + \epsilon_{87}^s \Gamma_{87}^{s,R}\right)$$
$$- \lambda_{s,R}^{LM}\left(\epsilon_{64}^s \Gamma_{64}^{s,L} + \epsilon_{53}^s \Gamma_{53}^{s,L}\right). \quad (37)$$

where $\epsilon_{ij}^s = \hbar\omega_{ij}^s$ expresses the energy level difference between the eigenstates $|i\rangle^s$ and $|j\rangle^s$.

B. Incoherent-correlated model mapping to the dark-state model

In this section, we discuss how the established incoherent-correlated model can be mapped to study dark-state formation. We assume that the system relaxations happen as in Fig. 6 under the conditions of resonance, $\omega_M^s - \omega_L^s = \omega_R^s$, ($s \in \{1, 2\}$). This creates two degenerate ground levels $|3\rangle^s$ and $|6\rangle^s$, and double-spin flip transitions happen with the same energy as single-spin flip transitions. We then find the transistor steady-state dynamics and energy flow rates. For transistor dark-state tuning, we let $\lambda_{s,P}^{QR} = 1$. We tune our system to a dark-state influenced by the work in Ref. [32]. Those authors elaborate on the ability to create different dark-states by changing the eigenvalues of the spectral density matrix γ_{kl}^s. Accordingly, the spectral density function can be written as a function of system-bath coupling constant $g_k^{s,l}$,

$$\gamma_{kl}^s = 2\pi g_k^{s,l}\left(g_k^{s,l}\right)^*.$$

The matrix γ_{kl}^s is Hermitian. If $g_k^{s,l}$ is real, then $\gamma_{kl}^s = \gamma_{lk}^s$. This makes $|\gamma_{kl}| = 0$, implying that there is at least one eigenvalue that is zero. We do a mapping from the correlated model to this under the approximations that the steady-state populations satisfy $\rho_{33}^s + \rho_{66}^s = 1$. With this assumption, other population densities become zero at the steady state. This condition allows us to tune the system to contain either $|6\rangle^s$ or $|3\rangle^s$ as dark-states by letting either $\gamma_{66}^s = 0$ or $\gamma_{33}^s = 0$. In a practical situation, this kind of relaxation will be influenced by the system-bath interactions explained in the beginning. They can be achieved via a resonator or a filter between the bath and the system. How to achieve such transitions is beyond the scope of the current paper and will be done in future work. To tune our incoherent system to contain $|6\rangle^s$ as the dark-state, we take $\gamma_{33}^s = 2\gamma(\omega)$ and $\gamma_{66}^s = 0$. This implies the restriction of relaxations from $|6\rangle^s$ and allowing twice the rate of relaxations as before from $|3\rangle^s$. Once we tune the transistor to contain this state, we observe that it is possible to switch on/off the transistor by changing the initial population density of $|6\rangle^s$ to 0/1, respectively.

We can change the bright-state and the dark-state by appropriately changing the restrictions and relaxations, and by allowing the transistors to be switched via the other lowest state, $|3\rangle^s$. Therefore, we can create both transistors to be controlled independently via either $|6\rangle^s$ or $|3\rangle^s$. We represent the transistor dynamics for our new model in Eq. (38) as

$$
\begin{aligned}
\dot{\rho}_{11}^s &= + \Gamma_{51}^{s,L} + 2\Gamma_{31}^{s,M} + \Gamma_{21}^{s,R}, \\
\dot{\rho}_{22}^s &= + \Gamma_{42}^{s,M} - \Gamma_{21}^{s,R} + 2\Gamma_{32}^{s,L}, \\
\dot{\rho}_{33}^s &= + 2\big(\Gamma_{73}^{s,L} - \Gamma_{31}^{s,M} + \Gamma_{43}^{s,R} - \Gamma_{32}^{s,L} + \Gamma_{83}^{s,M} + \Gamma_{53}^{s,R}\big), \\
\dot{\rho}_{44}^s &= + \Gamma_{84}^{s,L} - \Gamma_{42}^{s,M} - 2\Gamma_{43}^{s,R}, \\
\dot{\rho}_{55}^s &= - \Gamma_{51}^{s,L} + \Gamma_{75}^{s,M} - 2\Gamma_{53}^{s,R}, \\
\dot{\rho}_{66}^s &= 0, \\
\dot{\rho}_{77}^s &= - 2\Gamma_{73}^{s,L} - \Gamma_{75}^{s,M} + \Gamma_{87}^{s,R}, \\
\dot{\rho}_{88}^s &= - \Gamma_{84}^{s,L} - \Gamma_{87}^{s,R} - 2\Gamma_{83}^{s,M}.
\end{aligned}
\tag{38}
$$

We solve these equations of dynamics using MATHEMATICA V12 and confirm that at a steady state, the population of states has a proportionality to the initial condition of the dark-state. Since the equations are too complex to present here, we encourage the reader to refer to the supplemental material [47] and notice this dependence. When we tune a transistor to contain a dark-state $|6\rangle^s$, the steady-state populations represent

$$
\begin{aligned}
\rho_{11}^s &\propto \big[1 - \rho_{66}^s(0)\big], \\
\rho_{22}^s &\propto \big[1 - \rho_{66}^s(0)\big], \\
\rho_{33}^s &\propto \big[1 - \rho_{66}^s(0)\big], \\
\rho_{44}^s &\propto \big[1 - \rho_{66}^s(0)\big], \\
\rho_{55}^s &\propto \big[1 - \rho_{66}^s(0)\big], \\
\rho_{66}^s &= \rho_{66}^s(0), \\
\rho_{77}^s &\propto \big[1 - \rho_{66}^s(0)\big], \\
\rho_{88}^s &\propto \big[1 - \rho_{66}^s(0)\big].
\end{aligned}
\tag{39}
$$

We also obtain the heat flow rates for this as

$$
\begin{aligned}
J_L^s &= - \big(\epsilon_{51}^s \Gamma_{51}^{s,L} + + 2\epsilon_{73}^s \Gamma_{73}^{s,L} + \epsilon_{84}^s \Gamma_{84}^{s,L} + 2\epsilon_{32}^s \Gamma_{32}^{s,L}\big), \\
J_M^s &= - \big(2\epsilon_{31}^s \Gamma_{31}^{s,M} + \epsilon_{42}^s \Gamma_{42}^{s,M} + \epsilon_{75}^s \Gamma_{75}^{s,M} + 2\epsilon_{83}^s \Gamma_{83}^{s,L}\big), \\
J_R^s &= - \big(\epsilon_{21}^s \Gamma_{21}^{s,R} + 2\epsilon_{43}^s \Gamma_{43}^{s,R} + \epsilon_{87}^s \Gamma_{87}^{s,R} + 2\epsilon_{53}^s \Gamma_{53}^{s,L}\big).
\end{aligned}
\tag{40}
$$

C. Energy flow rates in the combined system

For the combined system, we apply the intermediate bath formalism introduced in Ref. [3]. Accordingly, at the intermediate bath junction, the rate of change of the intermediate bath's (B_I) average internal energy is equal to the sum of incoming and outgoing thermal flows and results in the equation

$$
\frac{dE_{\text{int}}^I}{dt} = J_R^1(t) - J_M^2(t).
\tag{41}
$$

Here J_R^1 is the energy flow rate from transistor 1 to B_I, and J_M^2 is the energy flow rate from B_I to transistor 2, as shown in Fig. 1. The exchange of the system with the surrounding baths is sustained over time, and it results in a nonequilibrium steady state. At this steady state, we get the heat flows for the combined model of the DP as

$$
\begin{aligned}
J_{\text{Leq}}(t) &= J_L^1(t) + J_L^2(t), \\
J_{\text{Meq}}(t) &= J_M^1(t), \\
J_{\text{Req}}(t) &= J_R^2(t).
\end{aligned}
\tag{42}
$$

The individual heat flow rates for each of the transistors are generalized, so we can combine as needed to realize different types of multitransistor models.

D. Nonequilibrium steady state and definition of temperature

The coupling strengths among the three TLSs can affect the physical picture that describes the quantum thermalization of the composite quantum system. When the coupling strengths among these subsystems are stronger than the system-bath couplings, the composite quantum system can be regarded as a single system. The dynamic evolution process of such a system approaching its steady state of thermal equilibrium can be understood as a nonequilibrium quantum thermalization [40].

The temperature for such a TLS composite system is defined based on any mixture of states ρ, formed with ground states ρ_g and excited states ρ_e (say, $\rho = \rho_g|g\rangle\langle g| + \rho_e|e\rangle\langle e|$), treated as a Gibbs state [40]. This is called an effective temperature, and it is defined using the ground state and the excited state as

$$
\frac{\rho_g}{\rho_e} = \exp\left(\frac{\hbar\omega}{k_B T}\right).
\tag{43}
$$

In our system, each of the transitions inside the system feels like a different temperature due to being coupled to baths with different temperatures. Thus, the system as a whole fails to come to a single temperature at equilibrium. As time passes, the system enters a nonequilibrium steady state. The system is irreversible at the nonequilibrium steady state and the entropy production is nonzero. We define an effective temperature according to Eq. (43) for a transition from $|j\rangle$ to $|k\rangle$ as

$$
T_{jk} = \frac{\hbar\omega_{jk}}{k_B \ln\left(\frac{\rho_{jj}}{\rho_{kk}}\right)}.
\tag{44}
$$

We can represent the ratio $\left(\frac{\rho_{jj}}{\rho_{kk}}\right)$ as in Eq. (27). This shows that each TLS is in thermal equilibrium with its directly coupled reservoir.

E. Device performance as an incoherent-correlated model

We use MATHEMATICA V12 to simulate the environmental effects on the multitransistor model. In all the simulations, we work in SI units. We take the reduced Planck constant as $\hbar = 1.055 \times 10^{-34}$ J s, the Boltzmann constant as $k_B = 1.381 \times 10^{-23}$ J/K, and the scaling factor for the frequencies as $\Delta = 1.3 \times 10^{11}$ Hz.
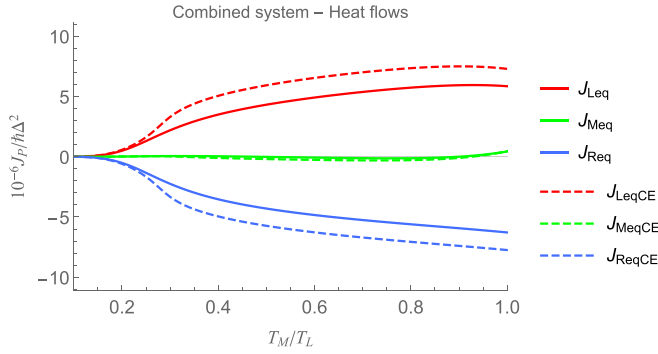
FIG. 8. This shows the combined energy flows in the DP. The solid lines show the equivalent heat flows J_{Leq}, J_{Meq}, and J_{Req} when we do not consider common environmental effects. The dashed lines show the equivalent heat flows J_{LeqCE}, J_{MeqCE}, J_{ReqCE} when we consider common environmental effects (i.e., when $\lambda_{s,P}^{QR} = 1$).

For the incoherent-correlated DP model, we visualize the following five scenarios:

Scenario 1: A fully common environmental case (i.e., all $\lambda_{s,P}^{QR} = 1$).

Scenario 2: No common environmental case (i.e., all $\lambda_{s,P}^{QR} = 0$).

Scenario 3: Hot, control baths and intermediate baths behaving as a common environment (i.e., $\lambda_{s,L}^{MR} = 1$, $\lambda_{1,R}^{LM} = \lambda_{2,M}^{RL} = 1$).

Scenario 4: Controlling bath and intermediate bath acting as a common environment (i.e., $\lambda_{1,M}^{RL} = 1$, $\lambda_{1,R}^{LM} = \lambda_{2,M}^{RL} = 1$).

Scenario 5: Middle and cold bath acting as a common environment (i.e., $\lambda_{2,R}^{LM} = \lambda_{2,M}^{MR} = 1$, $\lambda_{2,R}^{LM}$).

Figure 8 is a visualization of heat flows for scenario 1 and scenario 2 for a DP. In accord with the findings of Wijesekara *et al.* [9], the DP operates in the active region between the control temperatures $0.2T_L < T_M < 0.4T_L$. Our modeling also satisfies this range and is more suitable for working in the range $0.2T_L < T_M < 0.3T_L$ with an enhanced heat flow and thermal efficiency. Figure 9 gives the heat flow rate increase when the two transistors have slightly different characteristics with their angular frequencies such that $\omega_L^1 = 0.2\Delta$, $\omega_L^2 = 0.3\Delta\omega_M^s = 0$, $\omega_R^1 = 0.2\Delta$, $\omega_R^2 = 0.3\Delta\omega_{LM}^s = 0.9\Delta$, $\omega_{MR}^s = 1.1\Delta$, $\omega_{RL}^s = 0$, $T_L = 100$ mK, and $T_R = 30$ mK. Initially, we set the intermediate bath temperature as $T_I(0) = 30$ mK, and we vary T_M/T_L to observe the changes in heat flows. For the incoherent-correlated DP model, we tune the angular frequency parameters and observe J_{Leq} and J_{Req}, which act analogous to collector and emitter current on an electronic DP. In the DP operating region, we observe that it is possible to acquire more than a 50% increase in the heat flows at low temperatures, when $\lambda_{s,P}^{QR} = 1$. We also observe that at higher temperatures, this increase is only around 30–40 %. Let us discuss the performance of the modeled device using the overall thermal efficiency (TE) β for the heat flow into B_R. The equation for TE is given by

$$\beta = \frac{J_{\text{Leq}}}{J_{\text{Meq}}}. \tag{45}$$
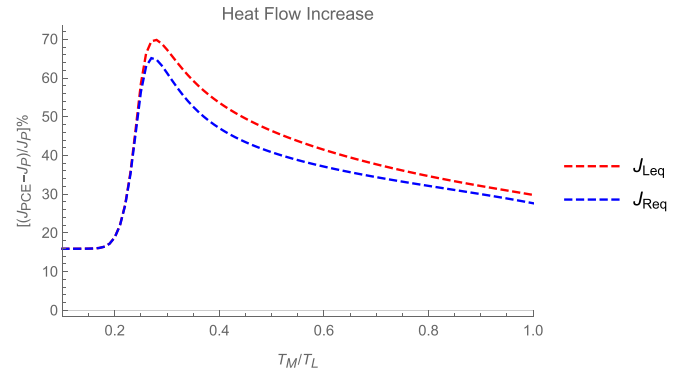
FIG. 9. We visualize the increase of J_{Leq} and J_{Req}, which act analogous to collector and emitter current on an electronic DP when there are environmental effects given by $\lambda_{s,P}^{QR} = 1$. The increase in the heat flows for the DP in the active operating region between $0.25T_L < T_M < 0.3T_L$ is more than 50%. We chose the two transistors with slightly different settings whose angular frequencies are selected at $\omega_L^1 = 0.2\Delta$, $\omega_L^2 = 0.3\Delta$, $\omega_M^s = 0$, $\omega_R^1 = 0.2\Delta$, $\omega_R^2 = 0.2\Delta$, $\omega_{LM}^s = 0.9\Delta$, $\omega_{MR}^s = 1.1\Delta$, $\omega_{RL}^s = 0$.

Figure 10 shows how TE changes for the DP with regard to the five scenarios. We also observe that the DP is ideal for operating in the lower control temperature T_M range to achieve a higher gain. We select the operating temperatures of the DP between $T_M = [0.2T_L, 0.3T_L]$. With the environmental effects, the gain increases drastically within this region. Thus, with an engineered environment, achieving a higher β value at a lower temperature is more possible than in the previous model. And for different scenarios, the rate at which the gain increases for changing temperature is different. We visualize how the thermal efficiency varies within the control temperature range $T_M = [0.22T_L, 0.28T_L]$ for various scenarios. Figure 11 shows that scenario 3 gives a very high thermal efficiency for the selected control temperature range. This implies that all the separate baths do not need to act as a common environment to achieve this enhancement.

To understand the influence of environmental coupling strengths, we visualize the change in the thermal efficiency
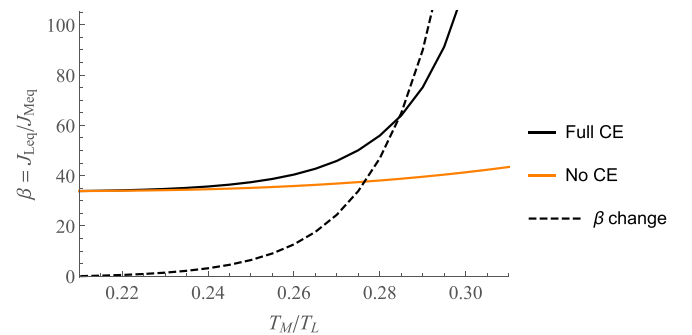
FIG. 10. The solid lines give the thermal efficiency of the DP operating in the control operating temperature range $T_M = [0.2T_L, 0.3T_L]$ for scenario 1 (Full CE) and 2 (No CE). The dashed lines show the efficiency increase as a percentage with respect to scenario 1 and scenario 2. The efficiency increase is exponential in this range indicating that higher efficiency can be achieved at a lower temperature by introducing common environmental effects.
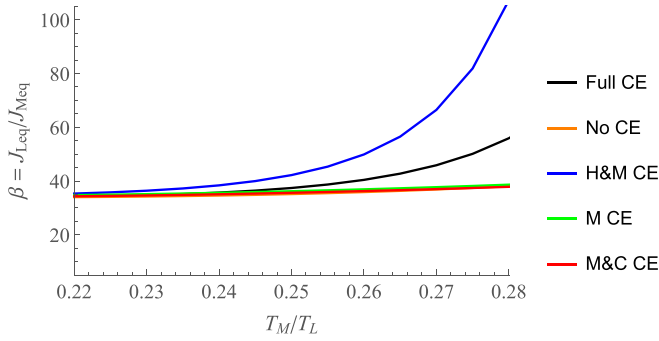
FIG. 11. Thermal efficiency values for different common environmental scenarios for the control temperature range $T_M = [0.22T_L, 0.28T_L]$ within the DP operating region. This shows how efficiency enhancement can be achieved in a far lower control temperature range than when there are no common environmental effects (no CE). Scenario 3 (H&M CE) gives a better performance for DP efficiency, implying that all baths do not need to act as a common environment to achieve this enhancement.

by adjusting $\lambda_{s,P}^{QR}$ between 0 and 1. As in Fig. 12, we achieve a higher efficiency when the coupling strength is maximum at $\lambda_{s,P}^{QR} = 1$. This analysis shows that we can engineer reservoir interactions so they enhance the device performance, which otherwise gets lost due to decoherence.

VII. THERMAL GATES FOR LOGIC OUTPUTS

Switching the transistors using temperatures is not feasible. The analysis in Ref. [9] demonstrated that it is possible to use an external optical field to control a transistor without changing its base terminal temperature. However, a complete switching off of the transistor using this method is impossible even if we remove the optical field completely for logic gate transistor arrangements. This is because the transitions that enable the transistor action can still be present via thermal bath interactions. We identify that with the tuned dark-state, a robust external channel opens up for transistor switching. The transistors can be switched on/off by changing the initial states
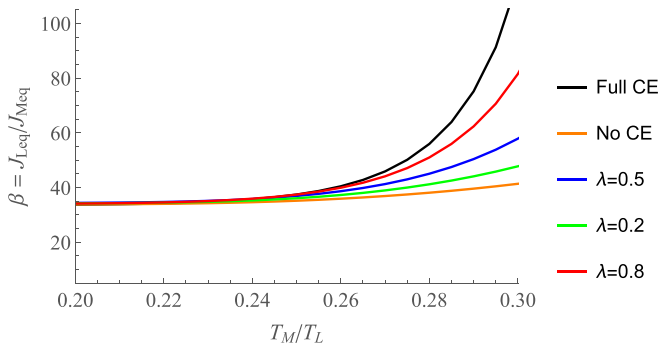
FIG. 12. Thermal efficiency for different common environmental couplings in the operating range $T_M = [0.2T_L, 0.3T_L]$. The efficiency increases as the magnitude of the coupling strength $\lambda_{s,P}^{QR}$ increases and a higher efficiency can be achieved in scenario 1 (Full CE). When $\lambda_{s,P}^{QR} = 0$, implying no CE is when the efficiency is lowest within this temperature range.
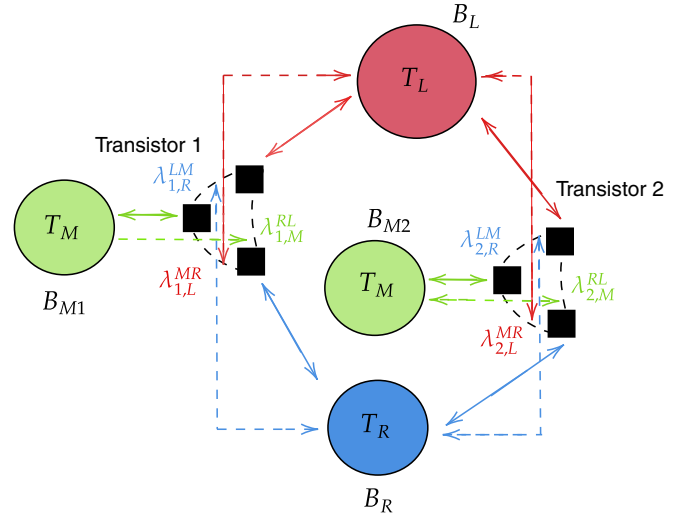
FIG. 13. OR gate multitransistor system. It comprises two similar transistors, having bath B_L with temperature T_L, two similar baths B_{M1} and B_{M2}, with the same temperature T_M and B_R with temperature T_R. A dark-state is formed due to direct interactions (solid lines) and indirect interactions (dashed lines) when $\lambda_{1,L}^{MR} = \lambda_{1,M}^{RL} = \lambda_{1,R}^{LM} = \lambda_{2,L}^{MR} = \lambda_{2,M}^{RL} = \lambda_{2,R}^{LM} = 1$.

of the dark-state populations' probability to 0/1. This concept shows potential in realizing the thermal analogous logic gates. This paper identifies the formation of gates using multitransistor arrangements and their outputs. We demonstrate a thermal counterpart for an electronic OR gate and an AND gate via dark-state switching.

The change of the initial population of the dark-state can be achieved using a laser field [34], which determines the transistor "ON" state and "OFF" state. For that, a laser field must drive the transitions between dark-state $|6\rangle$ (for the other transistor $|3\rangle$) to other excited states and change the populations accordingly. Since a dark-state is not influenced by thermal baths, it is possible to achieve this population change between the probabilities 0 and 1 using an external field. We approximate the time required for this state change to the Rabi frequency Ω. When the laser field frequency and the energy difference between the driving states are in resonance, we approximate the probability of state $|6\rangle$ (or $|3\rangle$ for the other transistor) achieving probabilities 0 and 1 as

$$P_{01}(t) = \sin^2\left(\frac{\Omega t}{2}\right).$$

Hence, the time until ρ_{66} (or ρ_{33}) reaches 1 or 0 will depend on t_d given as

$$t_d \approx \frac{\pi}{\Omega},$$

where $\Omega = \frac{\mathbf{E_0} \cdot \mathbf{d}}{\hbar}$, with electric field $|\mathbf{E_0}|$ and dipole moment $\mathbf{d}$ constant. When the time required for the system to reach the steady state (relaxation time) is τ_R, the switching time Δt of the transistors depends on

$$\Delta t = \max(t_d, \tau_R). \tag{46}$$
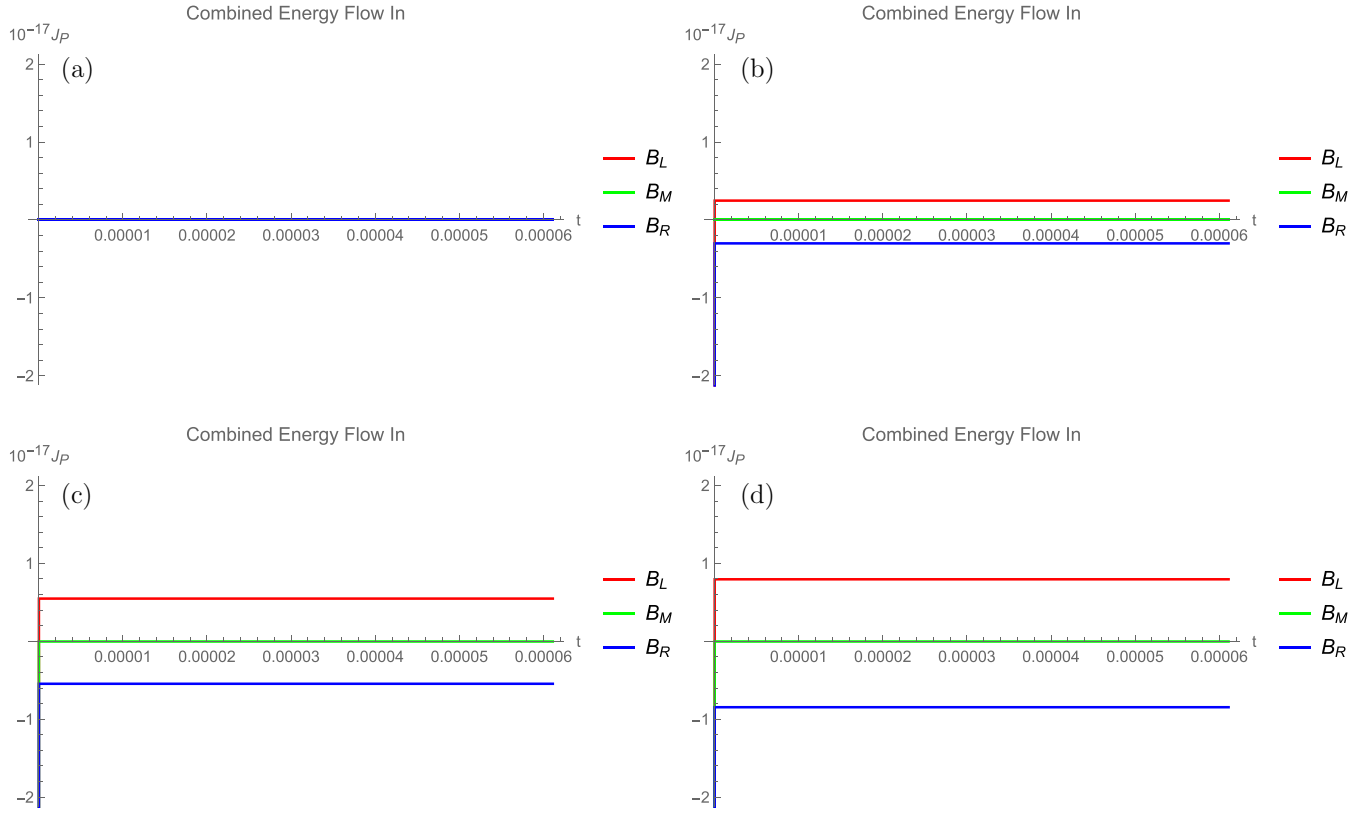
FIG. 14. OR truth for (a) both transistors "OFF" and the combined gate is also "OFF," (b) and (c) only one transistor is "ON" and the combined becomes "ON," and (d) both transistors are "ON" and the combined becomes "ON."

A. OR gate

We take all $\lambda_{s,P}^{QR} = 1$, and we tune transistor 1 to $|6\rangle$, and transistor 2 to $|3\rangle$ as their dark-states. This provides an independent state change for the two transistors. Since we do not expect any control from T_M, we keep it at a fixed temperature such that $T_L > T_M > T_R$ to enable the transistor action. We change the initial states of the dark-states manually in the program, and we observe that the switching time is approximately 8 ns. In the program, this depends only on the system relaxation time.

Figure 13 shows the arrangement of the two transistors similar to an electronic OR gate. We observe the combined model heat flows in the following four events.

Event 1: Both transistors "OFF."

Event 2: First transistor "OFF," second transistor "ON."

Event 3: First transistor "ON," second transistor "OFF."

Event 4: All transistors "ON."

At the steady state, Eq. (47) represents heat flows for the combined model to realize an OR gate as

$$
\begin{aligned}
J_{\text{Leq}}(t) &= J_L^1(t) + J_L^2(t), \\
J_{\text{Meq}}(t) &= J_M^1(t), \\
J_{\text{Req}}(t) &= J_R^1 + J_R^2(t).
\end{aligned}
\tag{47}
$$

The output results (see Table I and Fig. 14) give similar outputs to that of an electronic OR gate. Note that when the initial dark-state population probability is 0, the transistor is "ON," and when the initial dark-state population probability is 1, the transistor is "OFF." To resolve any confusion, we create

our logic convention similar to electronics, and we present the results in truth tables for "ON" as logic "1" and "OFF" as logic "0."

B. AND gate

Figure 15 shows the arrangement analogous to an electronic AND gate. We simulate the heat flow from the combined arrangement into the bath B_R corresponding to the previous four events. If there is a heat flow into B_R, we designate that to logic "1." We designate logic "0" if there is no heat flow into B_R. At the steady state, we consider the heat flows for the combined model for the AND gate as

$$
\begin{aligned}
J_{\text{Leq}}(t) &= J_L^1(t), \\
J_{\text{Req}}(t) &= J_R^2(t).
\end{aligned}
\tag{48}
$$

Figure 16 and Table II provide output results similar to the electronic AND gate. We observe that the switching time is around 8 ns.

TABLE I. OR truth table.

Transistor 1	Transistor 2	Combined gate
0	0	0
0	1	1
1	0	1
1	1	1
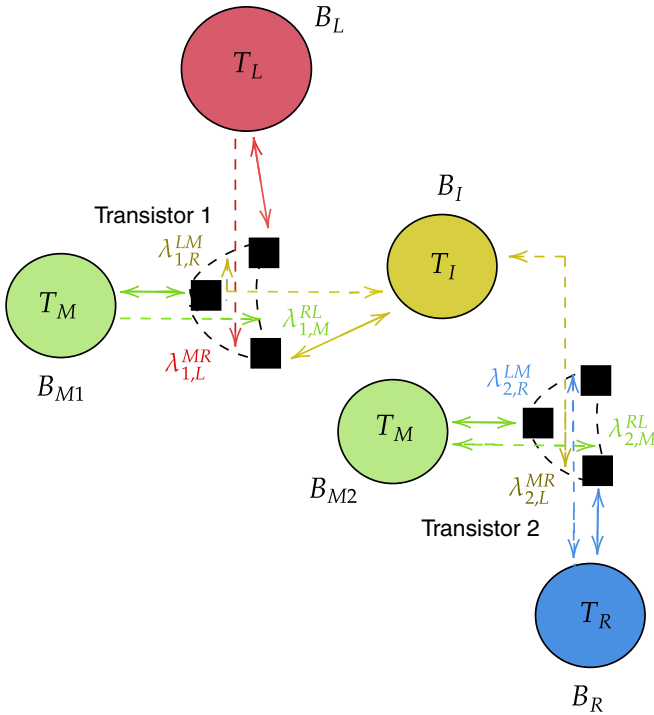
FIG. 15. AND gate arrangement. It comprises two similar transistors, having bath B_L with temperature T_L, two similar baths B_{M1} and B_{M2} with temperature T_M, B_R with temperatures T_R, and an intermediate bath B_I that links the two transistors. The intermediate bath temperature T_I depends on the internal transistor dynamics. A dark-state is formed due to direct interactions (solid lines) and indirect interactions (dashed lines) when $\lambda_{1,L}^{MR} = \lambda_{1,M}^{RL} = \lambda_{1,R}^{LM} = \lambda_{2,L}^{MR} = \lambda_{2,M}^{RL} = \lambda_{2,R}^{LM} = 1$.

VIII. CONCLUSIONS

In our previous work, where we analyzed a thermal transistor equivalent of an electronic Darlington pair (DP) [9], we needed enormous baths at the terminals to keep the temperatures regulated at preset temperatures and help the transistor action. The impact of such physically large baths coupled to two-level systems (TLSs) which act as the transistor terminals will not guarantee that the terminals are separated enough to avoid multiple interactions with the surrounding baths. When fabricating the device on a substrate, the multitransistor arrangements can have multiple interactions with the surrounding baths. These multiple interactions can suppress the heat flows or even completely obstruct the transistor action. Hence, mitigating or carefully engineering such interactions will be beneficial to keeping the transistor active and enhancing its performance. Throughout this analysis, we

TABLE II. AND truth table.

Transistor 1	Transistor 2	Heat flow into B_R
0	0	0
0	1	0
1	0	0
1	1	1

applied various environmental effect descriptions in the literature. We introduced an incoherent yet correlated model to a multitransistor system. This model is more generalized and can interpret the common environmental effects on the system by treating the common bath as separate baths. It also treat the single-spin flip and double-spin flip transitions induced by the baths independently. Then, we discussed the possibility of enhancing the thermal flow rates and producing a higher thermal efficiency, particularly for the DP model in its operating temperature range.

Finally, we discussed how an engineered environment is used to create new applications such as designing combinational logic. By introducing constraints, the incoherent model was tuned to contain dark-states. These dark-states are advantageous in providing external and independent switching to a multitransistor system. Unlike using an optical field in resonance to control a particular transition on the system, this provides a robust way to switch the transistor on/off, if required, periodically. Thus, we identified the possibility of realizing the functionality expected by an electronic AND gate and an OR gate. This work is also beneficial for realizing thermal equivalents of adder circuits, converters, and even sequential logic.

A. Limitations

The main limitation of our assumption is that the substrate behaves in a way that it can cause correlated system-bath interactions. For that, we need to consider a carefully engineered thermal bath as the substrate. And also, the system-environment couplings have to be very strong to see a more significant influence on the system by the common environmental effects. However, we used the Born-Markov and RWAs, assuming weaker couplings between the system and the reservoirs.

APPENDIX A: DERIVING THE QUANTUM MASTER EQUATION

Let us consider our system-bath interaction Hamiltonian $H_I(t)$ in the interaction picture given by

$$\hat{H}_I(t) = U^+(t, t_0)\hat{H}_I U(t, t_0). \tag{A1}$$

The Von-Neumann equation for the total density matrix $\rho_T(t)$ can be written as

$$\frac{d\hat{\rho}_T(t)}{dt} = -\frac{i}{h}[\hat{H}_I(t), \hat{\rho}_T(t)], \tag{A2}$$
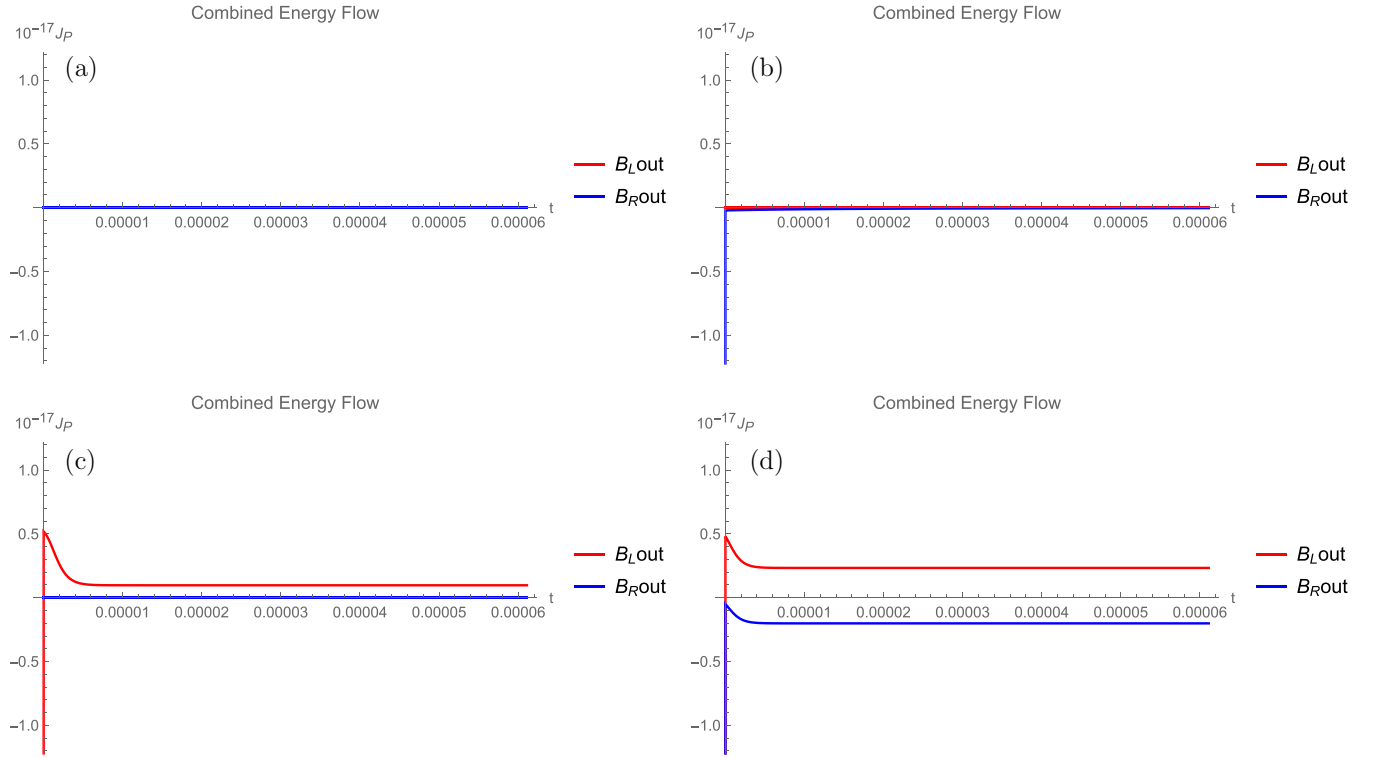
FIG. 16. AND truth for (a) both transistors "OFF" and there is no heat flow into B_R, (b) and (c) where only one transistor is "ON," and there is also no heat flow into B_R, and (d) is when both transistors are at "ON," ultimately showing heat flow into B_R.

which has the formal solution

$$\hat{\rho}_T(t) = \hat{\rho}_T(0) - \frac{i}{h} \int_0^t [\hat{H}_I(s), \hat{\rho}_T(s)] \, dt. \quad \text{(A3)}$$

Substituting the formal solution to the Von-Neumann equation again, we get

$$\frac{d\hat{\rho}(t)}{dt} = -\frac{i}{h}[\hat{H}_I(t), \hat{\rho}_T(0)] - \frac{1}{h^2} \int_0^t [\hat{H}_I(t), [\hat{H}_I(t), \hat{\rho}_T(s)]] \, ds. \quad \text{(A4)}$$

For the reduced density matrix, $\hat{\rho}(t) = \text{Tr}_B[\hat{\rho}_T(t)]$. The Von-Neumann equation reduces to

$$\frac{d\hat{\rho}(t)}{dt} = -\frac{i}{h}\text{Tr}_B[\hat{H}_I(t), \hat{\rho}_T(0)]$$
$$- \frac{1}{h^2} \int_0^t \text{Tr}_B[\hat{H}_I(t), [\hat{H}_I(s), \hat{\rho}_T(s)]] \, ds. \quad \text{(A5)}$$

For the two-transistor model, we assume that the two sets of three baths interact with two sets of the three TLSs, hence we define our system-bath interaction Hamiltonian as $\sum_P \hat{H}_{\text{sys-bath}}^s(t)$, where $P \in \{L, M, R\}$, and $s \in \{1, 2\}$. We further solve the Von-Neumann equation for two systems represented by "s" as

$$\frac{d\hat{\rho}_T(t)^s}{dt} = -\frac{i}{h}\left[\sum_P \hat{H}_{\text{sys-bath}}^{P,s}(t), \hat{\rho}_T^s(0)\right]$$
$$- \frac{1}{h^2} \int_0^t \left[\sum_P \hat{H}_{\text{sys-bath}}^{P,s}(t), [\hat{H}_{\text{sys-bath}}^{P,s}(t), \hat{\rho}_T^s(\tau)]\right] d\tau, \quad \text{(A6)}$$

where

$$\hat{\rho}_T^s = \hat{\rho}^s \otimes \hat{\rho}_L \otimes \hat{\rho}_M \otimes \hat{\rho}_R,$$
$$\hat{\rho}^s = \text{Tr}_P[\hat{\rho}_T^s].$$

Without loss of generality, $\text{Tr}_P[\sum_P \hat{H}_{\text{sys-bath}}^s(t), \hat{\rho}_T^s(0)] = 0$. Taking the partial trace over the reservoirs and performing Markovian approximations,

$$\frac{d\hat{\rho}^s(t)}{dt} = -\frac{1}{h^2}\text{Tr}_P \int_0^\infty \left[\sum_P \hat{H}_{\text{sys-bath}}^{P,s}(t), \left[\sum_Q \hat{H}_{\text{sys-bath}}^{Q,s}(t-\tau),\right.\right.$$
$$\left.\left. \times \; \hat{\rho}^s(t) \otimes \; \hat{\rho}_L \otimes \hat{\rho}_M \otimes \hat{\rho}_R \right]\right] d\tau. \quad \text{(A7)}$$

Let us consider the decomposition of the interaction Hamiltonian $\hat{H}_{\text{sys-bath}}^{P,s}(t)$,

$$\hat{H}_{\text{sys-bath}}^{P,s}(t) = \sum_{\omega, P} e^{-i\omega t} \hat{A}_P^s(\omega) \otimes B_P(t)$$
$$= \sum_{\omega, \alpha} e^{i\omega t} \hat{A}_P^{\dagger s}(\omega) \otimes B_P(t), \quad \text{(A8)}$$

such that the operators must satisfy

$$[\hat{H}_{\text{sys}}^s, A_P^s(\omega)] = \omega A_P^s(\omega),$$
$$[H_{\text{sys}}^s, A_P^s(-\omega)] = -\omega A_P^s(-\omega). \quad \text{(A9)}$$

Let us solve Eq. (A7). This comprises the trace terms

$$
\mathrm{Tr}_P\Bigg[\sum_P \hat{H}^{P,s}_{\text{sys-bath}}(t), \Bigg[\sum_Q \hat{H}^{Q,s}_{\text{sys-bath}}(t-\tau), \hat{\rho}^s(t) \otimes \hat{\rho}_L \otimes \hat{\rho}_M \otimes \hat{\rho}_R\Bigg]\Bigg]
$$

$$
= \mathrm{Tr}_B\Bigg[\hat{H}^{P,s}_{\text{sys-bath}}(t), \Bigg[\sum_Q \hat{H}^{Q,s}_{\text{sys-bath}}(t-\tau), \hat{\rho}^s(t) \otimes \hat{\rho}_B\Bigg]\Bigg] + \mathrm{Tr}_B[\hat{H}^{P,s}_{\text{sys-bath}}(t), [\hat{H}^{P,s}_{\text{sys-bath}}(t-\tau), \hat{\rho}^s(t) \otimes \hat{\rho}_B]], \tag{A10}
$$

but

$$
\mathrm{Tr}_{\mathrm{P,Q}}\big[\hat{H}^{P,s}_{\text{sys-bath}}(t), \big[\hat{H}^{Q,s}_{\text{sys-bath}}(t-\tau), \hat{\rho}^s(t) \otimes \hat{\rho}_P \otimes \hat{\rho}_Q\big]\big]
$$

$$
= \big[A^{\dagger s}_P(\omega)A^s_Q(\omega)\hat{\rho}^s(t) - A^s_Q(\omega)\hat{\rho}^s(t)A^{\dagger s}_P(\omega)\big]\mathrm{Tr}_{\mathrm{P}}[B_P(t)\hat{\rho}_P]\mathrm{Tr}_{\mathrm{Q}}\big[B_Q(t-\tau)\hat{\rho}_Q\big]. \tag{A11}
$$

However,

$$
\mathrm{Tr}_{\mathrm{P}}\big[\hat{H}^{P,s}_{\text{sys-bath}}(t), \hat{\rho}_P\big] = 0,
$$

$$
\mathrm{Tr}_{\mathrm{P}}[B_P(t)\hat{\rho}_P] = 0. \tag{A12}
$$

Therefore,

$$
\mathrm{Tr}_{\mathrm{P,Q}}\big[\hat{H}^{P,s}_{\text{sys-bath}}(t), \big[\hat{H}^{Q,s}_{\text{sys-bath}}(t-\tau), \hat{\rho}^s(t) \otimes \hat{\rho}_P \otimes \hat{\rho}_Q\big]\big] = 0. \tag{A13}
$$

Consider the expansion of $\mathrm{Tr}_B[\hat{H}^P_{\text{sys-bath}}(t)^s, [\hat{H}^P_{\text{sys-bath}}(t-\tau)^s, \hat{\rho}^s(t) \otimes \hat{\rho}_B]]$, which is the commutation relation to the same bath,

$$
\mathrm{Tr}_B\big[\hat{H}^{P,s}_{\text{sys-bath}}(t), \big[\hat{H}^{P,s}_{\text{sys-bath}}(t-\tau), \hat{\rho}^s(t) \otimes \hat{\rho}_B\big]\big] = \mathrm{Tr}_B\big[\big(\hat{H}^{P,s}_{\text{sys-bath}}(t)\hat{H}^{P,s}_{\text{sys-bath}}(t-\tau)\hat{\rho}^s(t)\hat{\rho}_B - \hat{H}^{P,s}_{\text{sys-bath}}(t-\tau)\hat{\rho}^s(t)\hat{\rho}_B\hat{H}^{P,s}_{\text{sys-bath}}(t)\big)
$$

$$
- \big(\hat{H}^{P,s}_{\text{sys-bath}}(t)\hat{\rho}^s(t)\hat{\rho}_B\hat{H}^{P,s}_{\text{sys-bath}}(t-\tau) - \hat{\rho}^s(t)\hat{\rho}_B\hat{H}^{P,s}_{\text{sys-bath}}(t-\tau)\hat{H}^{P,s}_{\text{sys-bath}}(t)\big)\big]. \tag{A14}
$$

Since our system comprises two similar transistors, the same set of equations repeats. Hence, we consider only one system ignoring s. Next, we consider the k mode expansion of Eq. (A15) by substituting decomposition terms, and this leads to the equation

$$
\mathrm{Tr}_B\big[\hat{H}^{P,s}_{\text{sys-bath}}(t), \big[\hat{H}^{P,s}_{\text{sys-bath}}(t-\tau), \hat{\rho}^s(t) \otimes \hat{\rho}_B\big]\big]
$$

$$
= \sum_{k,l}\sum_{\omega,\omega^*} e^{i(\omega^*-\omega)t}(A_l(\omega)\hat{\rho}(t)A^{\dagger}_k(\omega^*) - A^{\dagger}_k(\omega^*)A_l(\omega)\hat{\rho}(t))\int_0^{\infty} e^{i(\omega\tau)}\mathrm{Tr}_B[B^{\dagger}_k(t)B_l(t-\tau)\hat{\rho}_B]\,d\tau
$$

$$
+ \sum_{\omega,\omega^*} e^{-i(\omega^*-\omega)t}(\hat{\rho}(t)A_l(\omega)A^{\dagger}_k(\omega^*) - A^{\dagger}_k(\omega^*)\hat{\rho}A_l(\omega))\int_0^{\infty} e^{-i(\omega\tau)}\mathrm{Tr}_B[B^{\dagger}_k(t)B_l(t-\tau)\hat{\rho}_B]\,d\tau
$$

$$
= \sum_{k,l}\sum_{\omega,\omega^*} e^{-i\omega^*t}e^{-i\omega t}(A_l(\omega)\hat{\rho}(t)A^{\dagger}_k(\omega^*) - A^{\dagger}_k(\omega^*)A_l(\omega)\hat{\rho}(t))\int_0^{\infty} e^{i(\omega\tau)}TrB[B^{\dagger}_k(t)B_l(t-\tau)\hat{\rho}_B]\,d\tau + \mathrm{H.c.}, \tag{A15}
$$

where H.c. is the Hermitian conjugate. Define τ_s as the intrinsic evolution of the system given by

$$
\tau_s = \frac{1}{|\omega^*-\omega|},
$$

with the relaxation time of the system given by τ_R. Here we applied $A_k(\omega)$ terms for $\hat{H}_{\text{sys-bath}}(t-\tau)$ and $A^{\dagger}_k(\omega^*)$ for $\hat{H}_{\text{sys-bath}}(t)$. k and l represent the multiple components that interact with the Pth reservoir. When the coupling is weak, we need to consider only the resonant terms, following from the rotating wave approximation, $\omega^* = \omega$. Define $B_p(t) = \sum_k g_k(e^{-i\omega_k t}a^P_k + e^{i\omega_k t}a^{\dagger P}_k)$, which can be expanded further to

$$
[B^{\dagger}_k(t)B_l(t-\tau)\hat{\rho}_B] = g^*_k g_l\big[e^{i[\omega_k t-\omega_l(t-\tau)]}\big(a^{\dagger P}_k a^P_l\big) + e^{i[\omega_k t+\omega_l(t-\tau)]}\big(a^{\dagger P}_k a^{\dagger P}_l\big) + e^{-i[\omega_k t+\omega_l(t-\tau)]}\big(a^P_k a^P_l\big) + e^{-i[\omega_k t-\omega_l(t-\tau)]}\big(a^P_k a^{\dagger P}_l\big)\hat{\rho}_B\big]. \tag{A16}
$$

Taking the trace over the bath with only resonant terms,

$$
\mathrm{Tr}_B[B^{\dagger}_k(t)B_l(t-\tau)\hat{\rho}_B] = g^*_k g_l e^{-i[\omega_k t-\omega_l(t-\tau)]}\langle 0|a^P_k a^{\dagger P}_k|0\rangle
$$

$$
= |g_k|^2 e^{-i\omega_k \tau} \neq 0,
$$

and considering the integration, which is the Fourier transform,

$$\Gamma_{kl}(\omega) = \int_0^\infty e^{i\omega\tau} \mathrm{Tr}_B[B_k^\dagger(t)B_l(t-\tau)\hat\rho_B]\,d\tau. \tag{A17}$$

To divide the dynamics into Hermitian and non-Hermitian, Γ_{kl} is decomposed into

$$\Gamma_{kl}(\omega) = \tfrac{1}{2}\gamma_{kl}(\omega) + i\mathcal{S}_{kl}(\omega), \tag{A18}$$

where the Hermitian part is

$$\gamma_{kl}(\omega) = \Gamma_{kl}(\omega) + \Gamma_{kl}(\omega)^* = \int_{-\infty}^\infty e^{i(\omega\tau)} \mathrm{Tr}_B\big[B_k^+(t)B_l(t-\tau)\rho_B\big]\,d\tau. \tag{A19}$$

Considering only this dissipator term, we define the Lindblad term $\mathcal{L}_P^{kl}(\hat\rho(t))$ as

$$\mathcal{L}_P^{kl}(\hat\rho(t)) = \sum k,l \sum_\omega [(A_l(\omega)\hat\rho(t)A_k^\dagger(\omega) - A_k^\dagger(\omega)A_l(\omega)\hat\rho(t))\gamma_{kl}(\omega)/2 - (\hat\rho(t)A_k^\dagger(\omega)A_l(\omega) - A_l(\omega)\hat\rho A_k^\dagger(\omega))\gamma_{kl}(\omega)/2]$$

$$= \sum k,l \sum_\omega [2A_l(\omega)\hat\rho(t)A_k^\dagger(\omega) - (A_k^\dagger(\omega)A_l(\omega)\hat\rho(t) + \hat\rho(t)A_k^\dagger(\omega)A_l(\omega))]\gamma_{kl}(\omega)/2$$

$$= \sum k,l \sum_\omega \gamma_{kl}(\omega)\Big(A_l(\omega)\hat\rho(t)A_k^\dagger(\omega) - \frac{1}{2}\{A_k^\dagger(\omega)A_l(\omega), \rho(t)\}\Big). \tag{A20}$$

The matrix formed by the coefficients γ_{kl} is the Fourier transform of a positive function $\mathrm{Tr}B[B_k^+(t)B_l(t-s)\rho_B]$. If this can be diagonalized with a unitary operator, Γ_{kl} can be represented as

$$\Gamma_{kl}(\omega) = \delta_{kl}\big[\tfrac{1}{2}\gamma(\omega) + i\mathcal{S}(\omega)\big], \tag{A21}$$

where

$$\mathcal{S}(\omega) = -2\mathcal{P}\int_0^\infty \frac{\mathcal{J}(\omega)}{\omega}\,d\omega. \tag{A22}$$

In addition, $\mathcal{P}$ is the Cauchy principal part, and

$$\mathcal{J}(\omega) = \sum_k 2\pi|g_k|^2\delta(\omega - \omega_k). \tag{A23}$$

The dissipator part $\gamma(\omega)$ can be defined as

$$\gamma_\omega = 2\pi|g_k|^2\big(1 + n_p(\omega_k)\big)\int_{-\infty}^\infty e^{i(\omega-\omega_k)\tau}\,d\tau$$

$$+ 2\pi|g_k|^2 n_p(\omega_k)\int_{-\infty}^\infty e^{i(\omega+\omega_k)\tau}\,d\tau \tag{A24}$$

for $\omega < 0$,

$$\gamma_\omega = \mathcal{J}(-\omega)n_p(-\omega)$$

for $\omega > 0$,

$$\gamma_\omega = \mathcal{J}(\omega)(1 + n_p(\omega)),$$

where $n_P(\omega)$ is the Planck distribution given by

$$n_P(\omega) = \frac{1}{\exp\left(\frac{\hbar\omega}{k_B T_P}\right) - 1}. \tag{A25}$$

We simplify Lindblad terms to include only the direct coupling terms when $k = l = P$, where $P \in \{L, M, R, I\}$ for our model:

$$\mathcal{L}_P[\hat\rho(t)] = \sum_{\omega>0} \mathcal{J}(\omega)[1 + n_P(\omega)]\Big(A_P(\omega)\hat\rho(t)A_P^\dagger(\omega) - \frac{1}{2}\{A_P^\dagger(\omega)A_P(\omega), \hat\rho(t)\}\Big)$$

$$+ \sum_{\omega<0} \mathcal{J}(-\omega)n_P(-\omega)\Big(A_P(\omega)\hat\rho(t)A_P^\dagger(\omega) - \frac{1}{2}\{A_P^\dagger(\omega)A_P(\omega), \hat\rho(t)\}\Big)$$

$$= \sum_{\omega>0} \mathcal{J}(\omega)[1 + n_P(\omega)]\Big(A_P(\omega)\hat\rho(t)A_P^\dagger(\omega) - \frac{1}{2}\{A_P^\dagger(\omega)A_P(\omega), \hat\rho(t)\}\Big)$$

$$+ \sum_{\omega>0} \mathcal{J}(\omega)n_P(\omega)\Big(A_P(\omega)\hat\rho(t)A_P^\dagger(\omega) - \frac{1}{2}\{A_P^\dagger(\omega)A_P(\omega), \hat\rho(t)\}\Big). \tag{A26}$$

When we consider baths as separate, it is similar to analyzing the common environment in an independent bath regime. Thus, we get an incoherent correlated dissipation. For each of the transistors, there are six independent dissipative channels. Substituting everything back at Eq. (A7) and considering a multiquantum system (introducing "*s*"), we arrive at the

interaction picture master equation neglecting cross dissipation terms as

$$\frac{\partial \hat{\rho}^s(t)}{\partial t} = -\frac{i}{h}\left[\hat{H}^s_{LS}, \hat{\rho}^s(t)\right] + \sum_{P \in \{L,M,R\}} \mathcal{L}^s_P[\hat{\rho}^s(t)], \quad \text{(A27)}$$

where $\hat{H}^s_{LS}$ is the non-Hermitian part and is called the Lamb shift, given by

$$\hat{H}^s_{LS} = \sum_\omega \mathcal{S}^s(\omega) A^s_P(\omega) A^{\dagger s}_P(\omega). \quad \text{(A28)}$$

However, we neglect the Lamb shift assuming our system-system interactions to be negligible. This removes coherent evolution, and we can represent only the dissipative dynamics of the system using the master equation in the interaction picture as

$$\frac{\partial \hat{\rho}^s(t)}{\partial t} = \sum_{P \in \{L,M,R\}} \mathcal{L}^s_P[\hat{\rho}^s(t)]. \quad \text{(A29)}$$

[1] K. Joulain, J. Drevillon, Y. Ezzahri, and J. Ordonez-Miranda, Quantum Thermal Transistor, Phys. Rev. Lett. **116**, 200601 (2016).

[2] J. Ordonez-Miranda, Y. Ezzahri, and K. Joulain, Quantum thermal diode based on two interacting spinlike systems under different excitations, Phys. Rev. E **95**, 022128 (2017).

[3] R. T. Wijesekara, S. D. Gunapala, M. I. Stockman, and M. Premaratne, Optically controlled quantum thermal gate, Phys. Rev. B **101**, 245402 (2020).

[4] T. Werlang, M. A. Marchiori, M. F. Cornelio, and D. Valente, Optimal rectification in the ultrastrong coupling regime, Phys. Rev. E **89**, 062109 (2014).

[5] M. Majland, K. S. Christensen, and N. T. Zinner, Quantum thermal transistor in superconducting circuits, Phys. Rev. B **101**, 184510 (2020).

[6] J. Sun, X. Yuan, T. Tsunoda, V. Vedral, S. C. Benjamin, and S. Endo, Mitigating Realistic Noise in Practical Noisy Intermediate-Scale Quantum Devices, Phys. Rev. Appl. **15**, 034026 (2021).

[7] B.-q. Guo, T. Liu, and C.-s. Yu, Multifunctional quantum thermal device utilizing three qubits, Phys. Rev. E **99**, 032112 (2019).

[8] N. Gupt, S. Bhattacharyya, B. Das, S. Datta, V. Mukherjee, and A. Ghosh, Floquet quantum thermal transistor, Phys. Rev. E **106**, 024110 (2022).

[9] R. T. Wijesekara, S. D. Gunapala, and M. Premaratne, Darlington pair of quantum thermal transistors, Phys. Rev. B **104**, 045405 (2021).

[10] W. Zhu, I. D. Rukhlenko, and M. Premaratne, Light amplification in zero-index metamaterial with gain inserts, Appl. Phys. Lett. **101**, 031907 (2012).

[11] I. B. Udagedara, I. D. Rukhlenko, and M. Premaratne, Complex-ω approach versus complex-k approach in description of gain-assisted surface plasmon-polariton propagation along linear chains of metallic nanospheres, Phys. Rev. B **83**, 115451 (2011).

[12] D. Weeraddana, M. Premaratne, and D. L. Andrews, Quantum electrodynamics of resonance energy transfer in nanowire systems, Phys. Rev. B **93**, 075151 (2016).

[13] S. Mallawaarachchi, M. Premaratne, S. D. Gunapala, and P. K. Maini, Tuneable superradiant thermal emitter assembly, Phys. Rev. B **95**, 155443 (2017).

[14] H. Hapuarachchi, S. Mallawaarachchi, H. T. Hattori, W. Zhu, and M. Premaratne, Optoelectronic figure of merit of a metal nanoparticle—quantum dot (MNP-QD) hybrid molecule for assessing its suitability for sensing applications, J. Phys.: Condens. Matter **30**, 054006 (2018).

[15] H. Hapuarachchi and J. H. Cole, Influence of a planar metal nanoparticle assembly on the optical response of a quantum emitter, Phys. Rev. Res. **2**, 043092 (2020).

[16] T. Perera, S. D. Gunapala, M. I. Stockman, and M. Premaratne, Plasmonic properties of metallic nanoshells in the quantum limit: From single particle excitations to plasmons, J. Phys. Chem. C **124**, 27694 (2020).

[17] T. Perera, S. Mallawaarachchi, and M. Premaratne, Chiral plasmonic ellipsoids: An extended mie–gans model, J. Phys. Chem. Lett. **12**, 11214 (2021).

[18] A. Nisar, H. Hapuarachchi, L. Lermusiaux, J. H. Cole, and A. M. Funston, Controlling photoluminescence for optoelectronic applications via precision fabrication of quantum dot/au nanoparticle hybrid assemblies, ACS Appl. Nano Mater. **5**, 3213 (2022).

[19] Y. Liu, T. Perera, Q. Shi, Z. Yong, S. Mallawaarachchi, B. Fan, J. A.-T. Walker, C. J. Lupton, S. H. Thang, M. Premaratne, and W. Cheng, Thermoresponsive chiral plasmonic nanoparticles, Nanoscale **14**, 4292 (2022).

[20] K. Herath and M. Premaratne, Generalized model for the charge transport properties of dressed quantum hall systems, Phys. Rev. B **105**, 035430 (2022).

[21] K. Herath and M. Premaratne, Polarization effect on dressed plasmonic waveguides, Proc. SPIE **12274**, 122740Q (2022).

[22] C. Jayasekara, M. Premaratne, S. D. Gunapala, and M. I. Stockman, Mos$_2$ spaser, J. Appl. Phys. **119**, 133101 (2016).

[23] M. Premaratne and G. P. Agrawal, *Theoretical Foundations of Nanoscale Quantum Devices* (Cambridge University Press, Cambridge, 2021).

[24] A. Streltsov, U. Singh, H. S. Dhar, M. N. Bera, and G. Adesso, Measuring Quantum Coherence with Entanglement, Phys. Rev. Lett. **115**, 020403 (2015).

[25] P. R. Eastham, P. Kirton, H. M. Cammack, B. W. Lovett, and J. Keeling, Bath-induced coherence and the secular approximation, Phys. Rev. A **94**, 012110 (2016).

[26] Z.-Y. Zhou, M. Chen, L.-A. Wu, T. Yu, and J. Q. You, Dark state with counter-rotating dissipative channels, Sci. Rep. **7**, 6254 (2017).

[27] F. Galve, A. Mandarino, M. G. A. Paris, C. Benedetti, and R. Zambrini, Microscopic description for the emergence of collective dissipation in extended quantum systems, Sci. Rep. **7**, 42050 (2017).

[28] H. Liu, C. Wang, L.-Q. Wang, and J. Ren, Strong system-bath coupling induces negative differential thermal conductance and heat amplification in nonequilibrium two-qubit systems, Phys. Rev. E **99**, 032114 (2019).

[29] C. L. Latune, I. Sinayskiy, and F. Petruccione, Negative contributions to entropy production induced by quantum coherences, Phys. Rev. A **102**, 042220 (2020).

[30] S. Su, Y. Zhang, B. Andresen, and J. Chen, Coherence-enhanced thermal amplification for small systems, Physica A **569**, 125753 (2021).

[31] M. Cattaneo, G. L. Giorgi, S. Maniscalco, G. S. Paraoanu, and R. Zambrini, Bath-induced collective phenomena on superconducting qubits: Synchronization, subradiance, and entanglement generation, Ann. Phys. **533**, 2100038 (2021).

[32] B.-Q. Guo, N. N. Zhou, C. P. Yang, and C. S. Yu, Multifunctional quantum thermal device with initial-state dependence, Phys. E **142**, 115275 (2022).

[33] G. Manzano, G.-L. Giorgi, R. Fazio, and R. Zambrini, Boosting the performance of small autonomous refrigerators via common environmental effects, New J. Phys. **21**, 123026 (2019).

[34] Y.-Q. Liu, D.-H. Yu, and C.-S. Yu, Common environmental effects on quantum thermal transistor, Entropy **24**, 32 (2021).

[35] S. Alipour, F. Benatti, F. Bakhshinezhad, M. Afsary, S. Marcantoni, and A. T. Rezakhani, Correlations in quantum thermodynamics: Heat, work, and entropy production, Sci. Rep. **6**, 35568 (2016).

[36] S. Alipour, S. Tuohino, A. T. Rezakhani, and T. Ala-Nissila, Unreliability of mutual information as a measure for variations in total correlations, Phys. Rev. A **101**, 042311 (2020).

[37] A. Caldeira and A. Leggett, Quantum tunnelling in a dissipative system, Ann. Phys. **149**, 374 (1983).

[38] M. Cattaneo, G. L. Giorgi, S. Maniscalco, and R. Zambrini, Local versus global master equation with common and

separate baths: Superiority of the global approach in partial secular approximation, New J. Phys. **21**, 113045 (2019).

[39] L. Garziano, V. Macrì, R. Stassi, O. Di Stefano, F. Nori, and S. Savasta, One Photon Can Simultaneously Excite Two or More Atoms, Phys. Rev. Lett. **117**, 043601 (2016).

[40] G. M. Paule, *Thermodynamics and Synchronization in Open Quantum Systems* (Springer, Berlin, 2018).

[41] J.-Q. Liao, J.-F. Huang, and L.-M. Kuang, Quantum thermalization of two coupled two-level systems in eigenstate and bare-state representations, Phys. Rev. A **83**, 052110 (2011).

[42] Y.-J. Yang, Y. Q. Liu, and C. S. Yu, Heat transfer in transversely coupled qubits: optically controlled thermal modulator with common reservoirs, J. Phys. A **55**, 395303 (2022).

[43] H. P. Breuer and F. Petruccione, Quantum master equations, in *The Theory of Open Quantum Systems* (Oxford University Press, Oxford, 2007), pp. 109–218.

[44] Á. Rivas, A. D. K. Plato, S. F. Huelga, and M. B. Plenio, Markovian master equations: a critical study, New J. Phys. **12**, 113032 (2010).

[45] C. A. Brasil, F. F. Fanchini, and R. de Jesus Napolitano, A simple derivation of the lindblad equation, Rev. Bras. Ensino Fís. **35**, 01 (2013).

[46] R. Stárek, M. Mičuda, I. Straka, M. Nováková, M. Dušek, M. Ježek, J. Fiurášek, and R. Filip, Experimental quantum decoherence control by dark states of the environment, New J. Phys. **22**, 093058 (2020).

[47] See Supplemental Material at http://link.aps.org/supplemental/10.1103/PhysRevB.107.075440 for environmental transistor models.